KINETIC MECHANISM OF INDIGO-PRODUCING INDOLE MONOOXYGENASE

FROM *Acinetobacter baumannii*

Miss Kanyarat Suksomjaisaman

A Thesis Submitted in Partial Fulfillment of the Requirements

for the Degree of Master of Science in Biochemistry and Molecular Biology

Department of Biochemistry

FACULTY OF SCIENCE

Chulalongkorn University

Academic Year 2022

กลไกเชิงจลนศาสตร์ของอินโดลโมโนออกซีจีเนสที่ผลิตอินดิโกจาก *Acinetobacter baumannii*

น.ส.กัญญารัตน์ สุขสมใจสมาน

จุฬาลงกรณ์มหาวิทยาลัย
CHULALONGKORN UNIVERSITY

วิทยานิพนธ์นี้เป็นส่วนหนึ่งของการศึกษาตามหลักสูตรปริญญาวิทยาศาสตรมหาบัณฑิต
สาขาวิชาชีวเคมีและชีววิทยาโมเลกุล ภาควิชาชีวเคมี
คณะวิทยาศาสตร์ จุฬาลงกรณ์มหาวิทยาลัย
ปีการศึกษา 2565

Thesis Title   KINETIC MECHANISM OF INDIGO-PRODUCING INDOLE

                     MONOOXYGENASE FROM *Acinetobacter baumannii*

By   Miss Kanyarat Suksomjaisaman

Field of Study   Biochemistry and Molecular Biology

Thesis Advisor   Associate Professor SUPAART SIRIKANTARAMAS, Ph.D.

Thesis Co Advisor   Associate Professor JEERUS SUCHARITAKUL, D.D.S., PhD.

Accepted by the FACULTY OF SCIENCE, Chulalongkorn University in Partial Fulfillment of the Requirement for the Master of Science

.... Dean of the FACULTY OF SCIENCE

(Professor POLKIT SANGVANICH, Ph.D.)

THESIS COMMITTEE

.... Chairman

(Associate Professor KUNLAYA SOMBOONWIWAT, Ph.D.)

.... Thesis Advisor

(Associate Professor SUPAART SIRIKANTARAMAS, Ph.D.)

.... Thesis Co-Advisor

(Associate Professor JEERUS SUCHARITAKUL, D.D.S., PhD.)

.... Examiner

(KITTIKHUN WANGKANONT, Ph.D.)

.... External Examiner

(Assistant Professor Ruchanok Tinikul, Ph.D.)

กัญญารัตน์ สุขสมใจสมาน : กลไกเชิงจลนศาสตร์ของอินโดลโมโนออกซีจีเนสที่ผลิตอินดิโกจาก *Acinetobacter baumannii.* (KINETIC MECHANISM OF INDIGO-PRODUCING INDOLE MONOOXYGENASE FROM *Acinetobacter baumannii*) อ.ที่ปรึกษาหลัก : รศ. ดร.ศุภอรรจ ศิริกันทรมาศ, อ.ที่ปรึกษาร่วม : รศ. ทพ. ดร.จีรัสย์ สุจริตกุล

สารประกอบอินโดลมีโครงสร้างทางเคมีเป็น bicyclic ประกอบด้วยวงแหวนเบนซีนและไพโรลเชื่อมติดกัน ทำหน้าที่เป็นส่วนประกอบพื้นฐานในสารประกอบของธรรมชาติหลายชนิด นอกจากนี้อินโดลยังมีความสำคัญอย่างมากในการนำไปประยุกต์ใช้ในทางด้านอุตสาหกรรม โดยเฉพาะอย่างยิ่งอุตสาหกรรมในการผลิตยา และ เคมีการเกษตร โดยอินโดลเกิดปฏิกิริยาไฮดรอกซิเลชันที่มีเอนไซม์ออกซีจีเนสทำหน้าที่เป็นตัวเร่งปฏิกิริยาซึ่งมีบทบาทสำคัญในการสังเคราะห์สารประกอบเหล่านี้ โดยเกิดจากการทำงานร่วมกันของอินโดลโมโนออกซีจีเนสกับฟลาโวโปรตีนซึ่งเอนไซม์ทั้งสองชนิดนี้ทำให้เกิดกระบวนการไฮดรอกซิเลชันนี้ได้ ฟลาโวโปรตีนรีดักเตสคือ โปรตีนที่มี FAD เป็นโคแฟกเตอร์ ซึ่งรีดักเตสจะใช้ NADH ในการกระตุ้นปฏิกิริยารีดักชันของฟลาวินให้อยู่ในรูปของฟลาวินรีดิวซ์ และ ถูกถ่ายโอนไปยังส่วนของโมโนออกซีจีเนส จากนั้น โมโนออกซีจีเนสจะใช้อินโดลและออกซิเจนเป็นสารตั้งต้นสำหรับการเกิดปฏิกิริยาไฮดรอกซิเลชัน ในการศึกษานี้ เราโคลนอินโดลโมโนออกซีจีเนส (IndOx) จากจีโนมของ *Acinetobacter baumannii* และทำการโคลนลงในเวกเตอร์การแสดงออกพร้อมกับติด His-tag ที่ปลาย C-terminal การแสดงออกของ IndOx ทำให้ผลผลิตสูงถึง 0.31 กรัมต่อลิตร ในขณะที่รีดักเทส (IndR) ให้ผลผลิต 0.11 กรัมต่อลิตร ในอาหารเลี้ยงเชื้อ เพื่ออธิบายกลไกจลนศาสตร์ของเอนไซม์ ได้ดำเนินการโดยใช้เครื่องสเปกโตรโฟโตมิเตอร์แบบหยุดไหล พบว่าปฏิกิริยาไฮดรอกซิเลชันของอินโดลเกิดขึ้นเฉพาะที่ตำแหน่ง C3 ทำให้เกิดผลิตภัณฑ์ 3-ไฮดรอกซีอินโดล การทำความเข้าใจความซับซ้อนของกลไกการเกิดปฏิกิริยาในเอนไซม์รีคอมบิแนนท์จะช่วยทำให้สามารถผลิตสารประกอบอินดิกอยด์ สำหรับการใช้งานที่หลากหลาย เพื่อนำไปใช้ในทางการแพทย์ เครื่องสำอาง อุตสาหกรรมอาหาร และการผลิตวัสดุที่มีมูลค่าเพิ่มได้ในอนาคต

สาขาวิชา	ชีวเคมีและชีววิทยาโมเลกุล	ลายมือชื่อนิสิต ....
ปีการศึกษา	2565	ลายมือชื่อ อ.ที่ปรึกษาหลัก ....
		ลายมือชื่อ อ.ที่ปรึกษาร่วม ....

6372002123 : MAJOR BIOCHEMISTRY AND MOLECULAR BIOLOGY

KEYWORD: flavoprotein, two-component flavoprotein, flavoprotein monooxygenase, indole, indole monooxygenase, indigo

Kanyarat Suksomjaisaman : KINETIC MECHANISM OF INDIGO-PRODUCING INDOLE MONOOXYGENASE FROM *Acinetobacter baumannii*. Advisor: Assoc. Prof. SUPAART SIRIKANTARAMAS, Ph.D. Co-advisor: Assoc. Prof. JEERUS SUCHARITAKUL, D.D.S., PhD.

Indole, a bicyclic compound comprising a fused benzene and pyrrole ring, serves as a fundamental component in numerous natural compounds. Additionally, indole holds significant importance in industrial applications, particularly in the production of pharmaceutical drugs and agrochemicals. Flavin-dependent indole monooxygenase is an enzyme responsible for hydroxylation of the indole ring. Indole monooxygenase is a two-components: flavoprotein reductase containing FAD as a cofactor, and monooxygenase. The reductase component utilizes NADH to catalyze flavin reduction and transfers the reduced flavin to the monooxygenase component. The hydroxylation of indole by monooxygenase reduced FAD and oxygen as substrates. In this study, we cloned the indole monooxygenase (IndOx) from the genome of *Acinetobacter baumannii* and the gene was subcloned into an expression vector with a C-terminal histidine tag. The expression IndOx resulted in a high yield of 0.31 g/L, while reductase (IndR) yield of 0.11 g/L in the culture media. To elucidate the enzyme mechanism, rapid kinetic experiments were conducted using a stopped-flow spectrophotometer. The hydroxylation of indole was found a specific hydroxylation at the C3 position of indole ring, resulting in the production of 3-hydroxyindole. Understanding the enzyme reaction mechanism will be applied for enzyme engineering for production of indigoid compounds for diverse applications in medicines, cosmetics, food industries, and the manufacturing of high-value materials.

Field of Study:	Biochemistry and Molecular Biology	Student's Signature ....
Academic Year:	2022	Advisor's Signature ....
		Co-advisor's Signature ....

ACKNOWLEDGEMENTS

I would like to express my gratitude to all those who have contributed to the successful completion of this research project. First and foremost, I extend our deepest appreciation to our advisor, Assoc. Prof. Supaart Sirikantaramas, Ph.D., as well as co-advisor Assoc. Prof. Jeerus Sucharitakul, D.D.S., Ph.D., and for their guidance, support, and invaluable insights throughout the entire research process. Their expertise and encouragement have been instrumental in shaping this study. Second, I would like to thank Assoc. Prof. Teerapong Buaboocha, Ph.D., Assoc. Prof. Kulaya Somboonwiwat Ph.D., Assoc. Prof. Ruchanok Tinikul Ph.D., and Dr. Kittikhun Wangkanot for serving as my thesis committee members. The author is grateful to the Oral Biology Research Center, Faculty of Dentistry, Chulalongkorn University, and the laboratory of Assoc. Prof. Ruchanok Tinikul Ph.D., Faculty of Science, Mahidol University, for providing essential research equipment and facilities. Furthermore, we would like to acknowledge the individuals who generously participated in this study and provided valuable data and samples. Their cooperation and willingness to contribute have been vital in advancing our understanding in this field. Lastly, I extend our appreciation to my family. My friends include Konrawee is an elder who is always there to help, even when we have to stay overnight at the university, and I experience a mix of happiness and sadness in every moment with her., Aunchiya is my younger sister who delivers food and medicine. Additionally, she always provides support with university documents, and I loved ones for their unwavering support, understanding, and encouragement throughout this research journey. Their encouragement and belief in our abilities have been a constant source of motivation. Although it is impossible to mention everyone individually, we sincerely thank all those who have played a role, big or small, in the completion of this research project.

Kanyarat Suksomjaisaman

TABLE OF CONTENTS

Page

จุฬาลงกรณ์มหาวิทยาลัย
CHULALONGKORN UNIVERSITY

LIST OF TABLES

LIST OF FIGURES

Page

CHAPTER I

INTRODUCTION

Indigo is a deep blue dye that has been used for centuries to color fabrics, creating vibrant and enduring shades. It has a rich history, spanning various cultures and civilizations, and continues to be a popular dyeing agent in modern times. Indigo can be obtained through different methods, including extraction from plants, chemical synthesis, and fermentation by bacteria. This paper aims to provide an overview of indigo production methods, comparing the plant-based, bacterial, and chemical synthesis approaches.

Plant-based indigo production involves extracting the dye from plants belonging to the Indigofera genus, particularly Indigofera tinctoria and Indigofera suffruticosa. The leaves of these plants contain a chemical compound called indican, which is converted into indigo through a process known as "reduction." The leaves are soaked in water, fermented, and then oxidized to produce the insoluble blue pigment. This traditional method has been practiced for centuries, especially in countries like India, where indigo has played a significant role in their textile industry. Despite its historical importance, plant-based indigo production faces challenges such as land requirements, crop yield fluctuations, and environmental concerns related to large-scale cultivation (Qin et al., 2023).

An alternative method for indigo production involves the use of chemicals from petrochemical precursors. Chemical synthesis involves a series of complex reactions, typically starting with the aromatic compound aniline. Through multiple chemical transformations, aniline is converted into indigo. This method offers advantages in terms of scalability, consistency, and the ability to control the dye's properties. However, it is also associated with environmental concerns due to the use of petrochemicals and energy-intensive processes (Lai & Chang, 2021).

In addition to plant-based and chemical methods, indigo can also be synthesized by bacteria, specifically strains of the genus *Escherichia coli*. These bacteria are genetically modified to express enzymes that can convert the amino

acid tryptophan into indigo. This process, known as "biocatalysis," eliminates the need for extensive plant cultivation and offers the potential for more efficient and controlled production. Bacterial indigo production is a relatively recent development, with ongoing research and optimization efforts aiming to improve yields and scalability. Although this approach offers promising benefits in terms of sustainability and production control, it also raises concerns about genetically modified organisms (GMOs) and their potential ecological impacts (De Boer, 2014).

Each method has its advantages and challenges, with plant-based extraction being the traditional approach, chemical synthesis providing scalability and control, and bacterial fermentation offering potential sustainability benefits. As industries continue to evolve and prioritize sustainability, there is an ongoing exploration of new technologies and approaches to indigo production. Further research and development in these areas are essential for creating a more sustainable and environmentally friendly indigo dyeing industry.

However, the process of indigo biosynthesis by bacteria such as *Acinetobacter baumannii* has not been sufficiently studied in terms of enzyme kinetics and the mechanisms of indigo formation. In this research, both enzyme components will be subcloned into expression vectors with C-terminal His-tag. The kinetic mechanism will be elucidated by rapid kinetics using a stopped-flow spectrophotometer. Understanding the enzyme mechanism will lead to green chemistry using the biotechnological production of indigo instead of harsh chemical synthesis. Additional research and information pertaining to these subjects are thoroughly reviewed in this chapter, offering valuable insights, and further understanding of the topics.

1.1 Microorganisms that produce indigo.

Over the past few decades, numerous enzymes involved in indigo production have been found in microorganisms, predominantly in bacteria. In the past, the observation of indigo production was made while studying specific bacterial strains. However, in recent years, the identification of indigo-producing enzymes has been achieved through metagenome mining, a process that involves exploring the genetic material obtained from environmental samples. The discovery of these enzymes often occurred as an unintended outcome, as indicated by the pink or bluish coloration observed in colonies or cultures. These enzymes share the ability to convert indole through an oxygenation process. In most instances, this conversion relies on the presence of electron-donor cofactors and molecular oxygen, although there have been instances where peroxide-driven peroxygenases have been found to facilitate the conversion of indole to indigo. The identified redox enzymes can be categorized into three distinct enzyme classes based on the type of cofactor used for the oxygenation of indole: non-heme iron oxygenases, heme-containing oxygenases, and flavin-dependent monooxygenases (Fabara & Fraaije, 2020).

1.1.1 Non-heme iron oxygenase

The process of indigo formation is depicted in Figure 1, which illustrates the predicted reactions for all three pathways. Enzymes belonging to the non-heme iron oxygenase family, such as Napthalene dioxygenase from *Pseudomonas putida* G7, were utilized in the study. To facilitate the conversion of substrates like tryptophan, indole, and glucose into indigo, they were added to the medium. The achieved concentrations ranged from 36 to 300 mg/mL. It has been predicted that the enzyme follows the pathway depicted in Figure 1A for the process of indigo formation. The structure of this type of oxygenase is characterized by its alpha and beta subunits, forming a heterohexameric structure with the active site located in the alpha subunits. Within this group of enzymes, the non-heme iron cofactor is associated with Fe ligands, which are situated near two specific amino acids, histidine, and aspartate (Fabara & Fraaije, 2020; Groeneveld et al., 2016).
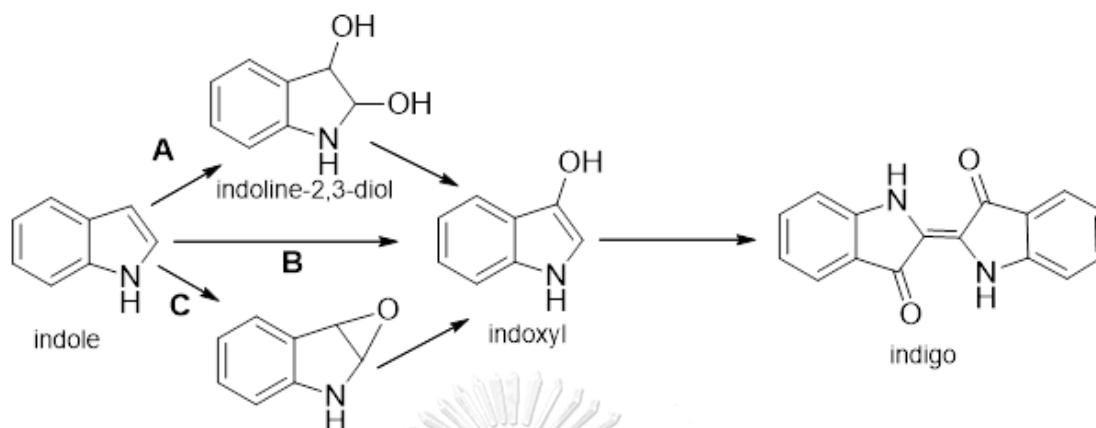
Figure 1. Indigo can be synthesized through different enzymatic pathways, which include deoxygenation.

(A), direct conversion through epoxidation (C), or hydroxylation leading to indoxyl (B). Modified from: Fabara AN, Fraaije MW. An overview of microbial indigo-forming enzymes. Applied Microbial Biotechnology. 2020;104(3):925-33.

Another enzyme, known as the multicomponent phenol hydroxylases from *Acinetobacter* sp. ST-550 possesses a hexameric hydroxylase structure consisting of three subunits $(\alpha\beta\gamma)_2$. In this reaction, flavoprotein reductase provides electrons to the oxygenase and cofactorless regulatory proteins. It has been reported that this enzyme produced 52 mg/mL of indigo in the culture broth. The indigo formation process predominantly follows pathway B as depicted in Figure 1.

1.1.2 Heme-containing oxygenases

In this group of enzymes, there are three major components involved in the reaction. One notable example is the Cytochrome P450 monooxygenase (CYPs) from *Bacillus megatherium* ATCC 14581, which consists of a heme redox cofactor, a flavin reductase domain, and a P450 monooxygenase domain. However, it is worth noting that reactions catalyzed by this enzyme in humans and other mammals tend to be slow, making it unsuitable for certain biotechnological processes. Unspecific peroxygenases belong to the class of heme-containing oxygenase, where the indigo

reaction occurs under reduced coenzyme conditions. In this process, electron donors such as NADH and NADPH are utilized, and non-essential cofactors are eliminated. The reactant in the reaction is hydrogen peroxide, which binds to the heme cofactor. Other enzymes that fall into this category include the marine dehaloperoxidase hemoglobin from *Amphitrite ornata* and the mammalian heme-containing indoleamine-2,3-dioxygenase (Fabara & Fraaije, 2020; Gillam et al., 2000).

1.1.3 Flavin-dependent monooxygenases

In this group, there are four main classes of flavoprotein monooxygenases (Fabara & Fraaije, 2020; Van Berkel et al., 2006), which are as follows: Most enzymes in the Styrene/Indole monooxygenase group are FAD-dependent and belong to class E of flavoprotein monooxygenases. These enzymes function as a two-component system, relying on the activities of both flavin reductase and monooxygenase. In most cases, these two enzymes are encoded by separate genes originating from the same DNA source. However, there are instances where genes that are physically linked to each other have been found. In this two-component process, the reductase is activated and reduced by NADH, after which it is transferred to the monooxygenase. When the two enzymes bind together, they can form an intermediate in the form of peroxyflavin, which reacts with oxygen. Some enzymes can undergo the peroxygenation pathway before proceeding to the hydroxylation pathway, resulting in the production of 52 mg/mL of indigo, as documented in the literature (Fabara & Fraaije, 2020; O'Connor et al., 1997; Panke et al., 1998; van Hellemond et al., 2007).

2-hydroxybiphenyl-3-monooxygenase is an FAD-dependent monooxygenase enzyme. However, the reaction does not occur under the influence of a reductase. Instead, it is catalyzed by a single-component enzyme belonging to the class A flavoprotein monooxygenase. In this class, the enzyme predominantly produces more indirubin than indigo (Fabara & Fraaije, 2020; Meyer et al., 2002).

Flavin-containing monooxygenases and Baeyer-Villiger monooxygenases. These enzymes belong to a group of enzymes characterized by their FAD-containing flavoprotein structure, classified as class B flavoproteins. These enzymes are primarily

found in the marine bacterium, Methylophaga aminisulfidivorans and exist as dimers. They exhibit reactivity with NADH and oxygen, demonstrating good catalytic activity with small aliphatic amines, sulphides, and indole substrates. Indigo production yields 911 mg/mL, while Corynebacterium glutamicum produces 685 mg/mL of indigo. Coexpression of Flavin-containing monooxygenase (FMO) with glucosyltransferase derived from Polygonum tinctorium leads to the production of 2.9 g/L indican. Additionally, type I Baeyer-Villiger monooxygenases can undergo oxidation reactions such as sulfoxidation, epoxidation, and N-oxidation (Fabara & Fraaije, 2020; Hsu et al., 2018). There are also alternative two-component flavoprotein monooxygenases that belong to class D flavoproteins. These enzymes have been identified in *Cupriavidus* sp. SHE and have demonstrated the ability to produce 307 mg/L of indigo (Dai et al., 2019; Fabara & Fraaije, 2020).

1.2 Indigo from *Acinetobacter baumannii*

Acinetobacter baumannii, a Gram-negative bacterium, has been reported to possess the capability to produce indigo. It is a ubiquitous microorganism found in various environmental sources, including soil, water, and hospital settings. *A. baumannii* is known for its versatility and adaptability, allowing it to survive in diverse conditions. The ability of *A. baumannii* to produce indigo can be advantageous in several ways. Firstly, indigo production by this bacterium offers a renewable and sustainable source of this valuable natural pigment. Unlike traditional methods that rely on plant extraction or chemical synthesis, microbial production can be more environmentally friendly and economically feasible. Additionally, *A. baumannii* can be easily cultivated and scaled up in laboratory conditions, making it a promising candidate for the industrial production of indigo (Antunes et al., 2011).

A. baumannii has the capability to produce indigo due to the presence of specific genes involved in the indigo synthesis pathway. One study focused on the *iifc* gene, which encodes a protein responsible for converting indole into indigo. The researchers analyzed the genome of *A. baumannii* and investigated the *iif* operon in comparison to that of *Pseudomonas syringae* p. *actinidiae*. By studying these genetic

components, they aimed to gain insights into the specific mechanisms underlying indigo production in *A. baumannii*. In this study, it was identified that tryptophan serves as an amino acid derivative of indole.

Indole and its derivatives form a significant category of heterocyclic aromatic compounds that have extensive applications in pharmaceutical synthesis, dye production, and industrial solvent manufacturing (Arora et al., 2015; Sumpter W. C., 1954). Indole and its derivatives can be found in various natural sources. L-tryptophan, a crucial amino acid found in the majority of proteins, undergoes microbial metabolism to produce indole, a significant byproduct (Arora et al., 2015; Mohammed et al., 2003; Yokoyama & Carlson, 1974). More than 85 species of bacteria, including both Gram-positive and Gram-negative, have the ability to synthesize indole (Lee & Lee, 2010). Due to its toxicity and widespread dispersion in a variety of ecosystems, including soils, coastal regions, groundwater, surface waters, and even interior settings, indole and its derivatives are regarded as environmental pollutants (Arora et al., 2015; Fetzner, 1998; Gu & Berry, 1992). There is a dearth of literature on the microbial breakdown of indole, despite the fact that several reviews have been written about its uses and microbial synthesis (Lee & Lee, 2010; Yuan et al., 2011). Indole concentrations as high as 3.5 mM have been shown to exert a potent inhibitory effect on wild-type *A. baumannii*. However, when the indole concentrations remain below 3.5 mM, bacterial cells are still able to maintain their viability, potentially through the oxidation of indole to indigo (Lin et al., 2015). (Figure 2.)
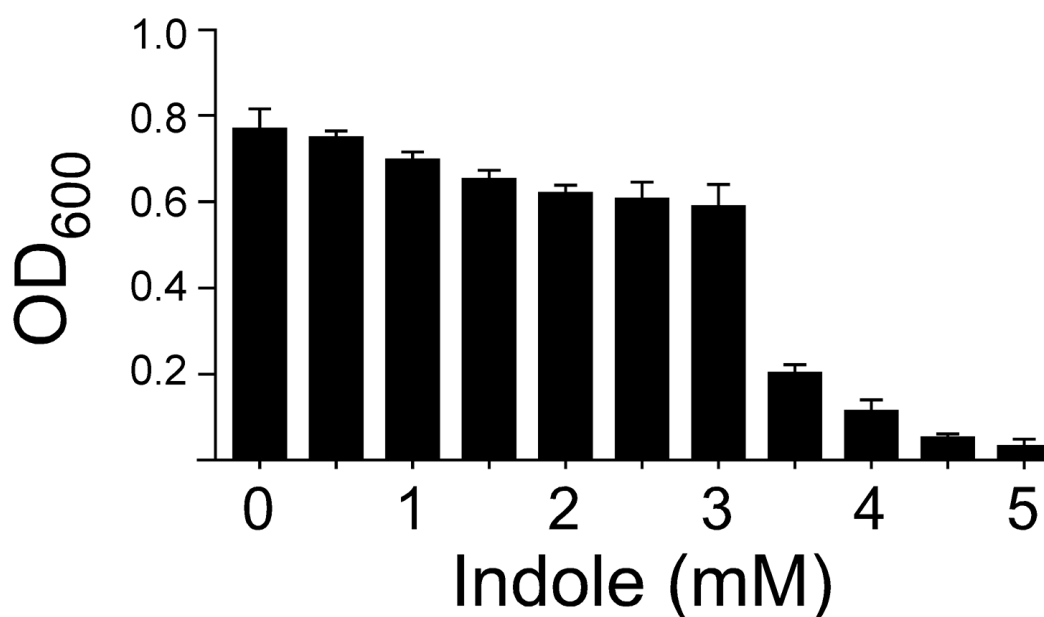
Figure 2. The impact of indole on the growth of wild-type A. baumannii ATCC 19606

It was investigated by cultivating the bacteria in M9 medium supplemented with varying concentrations of indole (ranging from 0 to 6 mM) for a duration of 16 hours. Taken from: Lin GH, Chen HP, Shu HY. Detoxification of Indole by an Indole-Induced Flavoprotein Oxygenase from *Acinetobacter baumannii*. (Lin et al., 2015)

In both *A. baumannii* and *Pseudomonas syringae* pv. *actinidiae*, the *iif* (indole induced flavoprotein) operon has been found to be activated by indole through the AraC-like transcriptional regulator *iifR*. The *iifd* gene is situated immediately downstream of *iifc*, and its expression is influenced by *iifR*. Since *iifR* belongs to the AraC/XylS family, it plays a crucial role in regulating carbon metabolism, stress response, and pathogenesis. Additionally, it serves as a key regulator of the *iif* operon, controlling its expression. However, the primary factor influencing the production of indigo or indigo resistance is primarily associated with the *iifc* gene, which acts synergistically with the flavoprotein *iifd* gene (Lin et al., 2015). (Figure 3.)
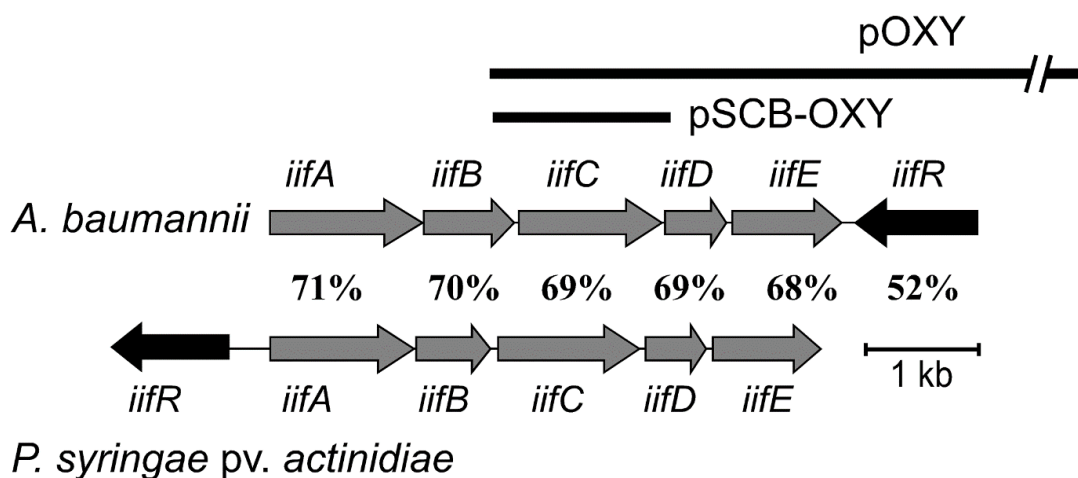
Figure 3. The gene organization of the *iif* operon in *A. baumannii* ATCC 19606 and *P. syringae* pv. *actinidiae* ICMP 19070.

There is illustrated in the diagram. In *A. baumannii* ATCC 19606, the *iif* operon consists of five genes, represented by gray arrows, namely *iifA*, *iifB*, *iifC*, *iifD*, and *iifE*. The dark-gray arrow represents the AraC-like regulator *IifR*. The inserts of pOXY and pSCB-OXY are indicated by thick lines. The locus_tags for the genes in *A. baumannii* ATCC 19606 are F911_02006, F911_02005, F911_02004, F911_02003, F911_02002, and F911_02001 for *iifA*, *iifB*, *iifC*, *iifD*, *iifE*, and *iifR*, respectively. In *P. syringae* pv. *actinidiae* ICMP 19070, the locus_tags for the corresponding genes are A259_30100, A259_30105, A259_30110, A259_30115, A259_30120, and A259_30095, respectively. Taken from: Lin GH, Chen HP, Shu HY. Detoxification of Indole by an Indole-Induced Flavoprotein Oxygenase from *Acinetobacter baumannii*. (Lin et al., 2015)

1.3 Flavoprotein monooxygenase

Flavoprotein monooxygenases (FPMOs) play various roles in biological processes, including lignin degradation, natural product biosynthesis, and detoxification of xenobiotic compounds. These enzymes rely on a flavin mononucleotide (FMN) or flavin adenine dinucleotide (FAD) cofactor to activate molecular oxygen (O_2). By incorporating one atom of O_2 into the substrate and reducing the other oxygen atom to water, FPMOs facilitate O_2 activation. This process typically involves the formation of a covalent adduct between the two-electron reduced flavin cofactor and the O_2 molecule. As a result, FPMOs transiently stabilize the flavin C4a-(hydro)peroxide species, which can exhibit nucleophilic or electrophilic reactivity towards the substrate depending on its protonation state (Paul et al., 2021). (Figure 4.)
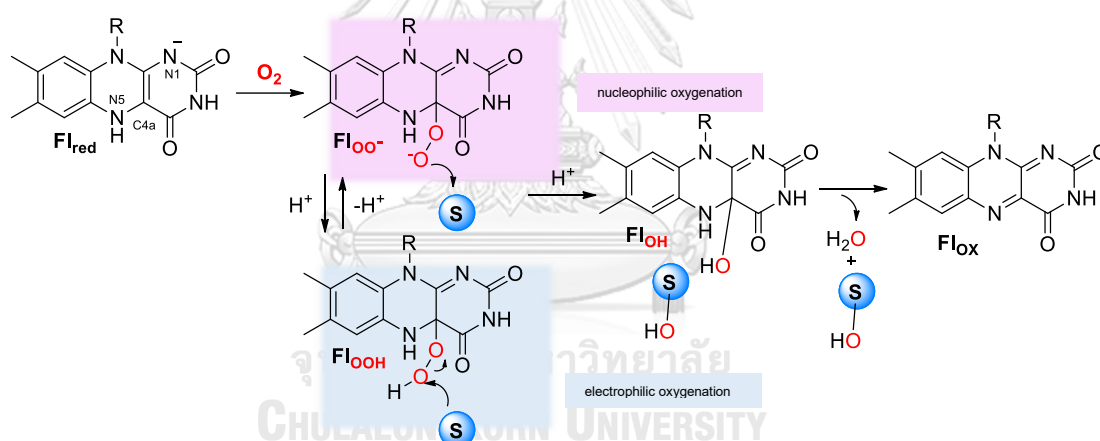
Figure 4. FPMOs form covalent adducts between flavin and oxygen during their catalytic process.

When the reduced form of flavin (Fl_{red}) interacts with molecular oxygen (O_2), it forms a covalent adduct known as flavin C4a-(hydro)peroxide ($Fl_{OO(H)}$). This adduct can then react with a substrate (S) to produce a product (SOH) and flavin C4a-hydroxide (Fl_{OH}). The Fl_{OH} molecule eventually decomposes, releasing water, and resulting in the formation of oxidized flavin (Fl_{ox}). Modified from: Lin GH, Chen HP, Shu HY. Detoxification of Indole by an Indole-Induced Flavoprotein Oxygenase from *Acinetobacter baumannii.* (Lin et al., 2015)

The initial classification of FPMOs was introduced in 2006, distinguishing them into six groups based on their unique structural and functional characteristics. The groups included single-component enzymes that utilize NAD(P)H as an external electron donor (groups A and B), as well as two-component enzymes that rely on a flavin reductase for electron transfer (groups C to F, as shown in Table 1). Subsequently, in 2014, two additional groups, G and H, were added to the classification, which encompasses self-sufficient FPMOs that can internally generate the necessary electrons and do not require an external electron donor (Paul et al., 2021).

Table 1. Classification of FPMOs

Group	Flavin-binding domain	CATH code	Cofactor	Electron donor	Prototype reaction
A	three-layer ββα sandwich	3.50.50.60	FAD	NAD(P)H	aromatic hydroxylation
B	three-layer ββα sandwich	3.50.50.60	FAD	NAD(P)H	Baeyer-Villiger oxidation
C	TIM-barrel	3.20.20.30	FMN	$FMNH_2$	light emission
D	acyl-CoA dehydrogenase	1.10.540.10	FAD/FMN	$FADH_2/FMNH_2$	aromatic hydroxylation
E	three-layer ββα sandwich	3.50.50.60	FAD	$FADH_2$	epoxidation
F	three-layer ββα sandwich	3.50.50.60	FAD	$FADH_2$	oxidative halogenation
G	three-layer ββα sandwich	3.50.50.60	FAD	Substrate	oxidative deamination
H	TIM-barrel	3.20.20.70	FMN	Substrate	oxidative decarboxylation

The groups of FPMOs are assigned different colors according to the CATH (Class, Architecture, Topology, and Homologous superfamily) classification of their flavin binding domain (Mascotti et al., 2016).

1.3.1 Group A of flavoprotein monooxygenases

Group A FPMOs primarily function as aromatic hydroxylases. They consist of a Rossmann-like three-layer ββα sandwich domain responsible for binding the FAD cofactor and a substrate domain rich in β-strands. Members of Group A exhibit mobility of the flavin cofactor and bind the NAD(P)H coenzyme in a groove on the protein surface. They can be distinguished from other FAD-dependent FPMOs by their conserved FAD-NAD(P)H binding motif, known as the DG fingerprint. Another notable characteristic of Group A FPMOs is the regulatory role of the substrate, which enhances flavin reduction and facilitates the release of NAD(P)$^+$.

1.3.2 Group B of flavoprotein monooxygenase

Group B FPMOs primarily include Baeyer-Villiger monooxygenases (Type I BVMOs) and heteroatom oxygenases. These enzymes feature a Rossmann-like three-layer ββα sandwich domain for FAD binding, similar to Group A FPMOs. In Group B FPMOs, the substrate is bound after flavin reduction, and NAD(P)+ remains bound during substrate oxidation. To facilitate this process, Group B enzymes possess a separate three-layer ββα sandwich domain specifically designed for binding the pyridine nucleotide.

1.3.3 Group C of flavoprotein monooxygenase

Group C FPMOs are responsible for catalyzing various types of oxygenation reactions. They possess a luciferase-like TIM-barrel fold, which enables them to bind FMNH2.This group includes enzymes such as pyrimidine monooxygenase, dibenzothiophene sulfone monooxygenase, and hexachlorobenzene monooxygenase. These enzymes are known to form a flavin N5-(per)oxide intermediate during their catalytic cycle.

1.3.4 Group D of flavoprotein monooxygenase

Group D FPMOs are involved in various oxygenation reactions and have diverse substrate specificities. They can utilize either $FMNH_2$ or $FADH_2$ as electron donors, and their structure is characterized by an acyl-CoA dehydrogenase fold.

1.3.5 Group E and F of flavoprotein monooxygenase

Group E and F FPMOs consist of epoxidases and halogenases, respectively. These groups share similarities with group A FPMOs, including the presence of a three-layer ββα sandwich domain. However, they differ in their C-terminal sequences.

1.3.6 Group G and H of flavoprotein monooxygenase

Group G and H FPMOs are single-component enzymes that perform flavin cofactor reduction through substrate oxidation. They are primarily involved in oxidative deamination and oxidative decarboxylation reactions. Group G enzymes possess a three-layer ββα sandwich domain, as well as a monoamine oxidase-like domain and a C-terminal α-helix domain. On the other hand, group H enzymes feature a type I aldolase-like TIM-barrel domain for binding FMN.

This study reports the presence of indole monooxygenase or styrene monooxygenase, which belongs to group E of enzymes. Additionally, some modifications or additional features have been identified in these enzymes. Flavin reductase-dependent monooxygenases, referred to as group E FPMOs, possess a FAD-binding domain that bears resemblance to the FAD-binding domain found in group A enzymes. These enzymes rely on a flavin reductase to supply them with the reduced form of FAD necessary for their monooxygenase function. Certain group E FPMOs are self-sufficient enzymes due to their natural fusion of the oxygenase and reductase domains. Group E can be further divided into two subgroups based on distinctive sequence motifs present in their active sites. Subgroup E1 includes styrene monooxygenase (SMO), which exhibits a preference for styrene derivatives as substrates. Conversely, subgroup E2 comprises indole monooxygenases (IMO) that display the highest activity with indole derivatives. Please note that the provided paraphrase retains the original structure and content of the information while addressing any grammar concerns.

In terms of mechanism, group E enzymes employ an electrophilic attack by the flavin C4a-hydroxyperoxide intermediate (Figure 5). This intermediate reacts with either a carbon double bond in epoxidation reactions or the lone pair of electrons on a sulfur atom in heteroatom oxidations, acting as the nucleophile in each case. Reduced FAD is supplied by the corresponding reductase and taken up by the oxygenase in a manner similar to that observed in group D enzymes. Substrate binding occurs subsequent to the formation of the flavin oxygenation species. Once the highly fluorescent flavin C4a-hydroxide decomposes, the product and oxidized cofactor are released. While the interaction between SMO's oxygenase and reductase is described as weak, studies on enzymes from *Pseudomonas* and *Rhodococcus* have demonstrated that the presence of the reductase enhances the catalytic activity of the oxygenase, indicating that the interaction with the reductase promotes overall epoxidase activity. The fusion proteins mentioned earlier represent a unique scenario where the reductase and oxygenase domains interact obligatorily. This paraphrase maintains the original information's core meaning while addressing grammatical concerns (Sucharitakul et al., 2008).

Reduced flavin   **C(4a)-hydroperoxyflavin**   **Oxidized flavin**
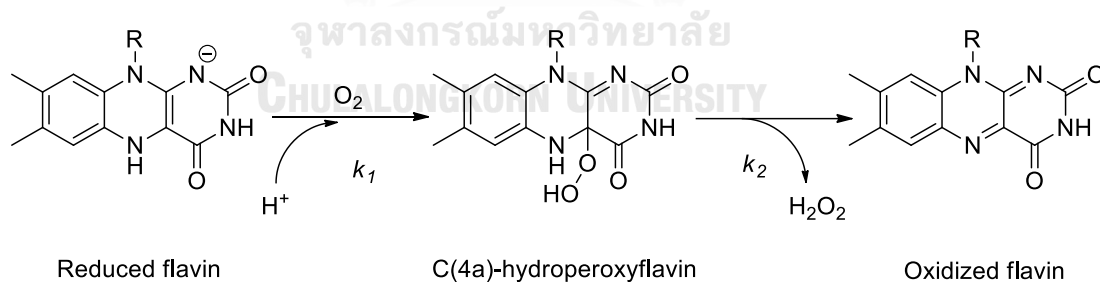
Figure 5 The reaction of reduced flavin with oxygen forming C4a-hydroproxyflavin intermediate.

Modified from: Sucharitakul J, Prongjit M, Haltrich D, Chaiyen P. Detection of a C4a-hydroperoxyflavin intermediate in the reaction of a flavoprotein oxidase. Biochemistry. 2008;47(33):8485-90.

According to current understanding, this system demonstrates the most efficient oxygenation rate among two-component FPMOs in practical biocatalysis applications. Furthermore, group E enzymes have the ability to convert a wide range of substituted aromatic and aliphatic alkenes, as well as oxidize aromatic sulfides, sulfanes, and benzothiophenes. This paraphrase maintains the original information's essence while addressing grammatical concerns.

1.4 Single-component and two-component enzyme

Phenolic acids, which belong to the aromatic compound family, are abundant in nature and play a significant role in various applications across industries such as chemicals, agriculture, food, and pharmaceuticals. They are found in lignocellulose, natural products, and synthetic chemicals. Phenolic acids exhibit diverse biological activities including antioxidant, anticancer, antimicrobial, antifungal, and anti-inflammatory properties, making them valuable in pharmaceutical and food sectors. The introduction of hydroxyl groups to phenolic acids generally enhances their radical scavenging ability and other biological activities. For instance, 3,4,5-trihydroxycinnamic acid (3,4,5-THCA), 3,4,5-trihydroxyphenylacetic acid (3,4,5-THPA), and gallic acid have been shown to possess stronger antioxidant and anti-inflammatory effects compared to their non-hydroxylated counterparts. Therefore, enzymatic hydroxylation of phenolic acids plays a crucial role in enhancing their biological activities.

Four types of enzymes have been identified as catalysts for aromatic hydroxylation: cytochrome P450, non-heme iron, pterin-dependent, and flavin-dependent monooxygenases. This review focuses specifically on flavin-dependent systems and aims to provide a comprehensive understanding of their mechanisms. These flavin-dependent monooxygenases can be categorized into two types:

- The first type functions as a single-component monooxygenase, where the enzyme binds to flavin (in its oxidized form, FAD) as a prosthetic group.

- The second type operates as a two-component monooxygenase, wherein the enzyme does not tightly bind to oxidized flavin but instead relies on reduced flavin supplied by a separate reductase enzyme.

This review will delve into the mechanistic details of these representative flavin-dependent monooxygenases that specifically catalyze the hydroxylation of aromatic compounds or perform hydroxylation alongside additional reactions. Additionally, the challenges associated with their practical application will be discussed.

1.4.1 Single-component flavin-dependent monooxygenases

The reaction cycle of single-component flavin-dependent monooxygenases involved in aromatic hydroxylation can be separated into two distinct phases: the reductive half-reaction and the oxidative half-reaction (Figure 6) (Chenprakhon et al., 2019).
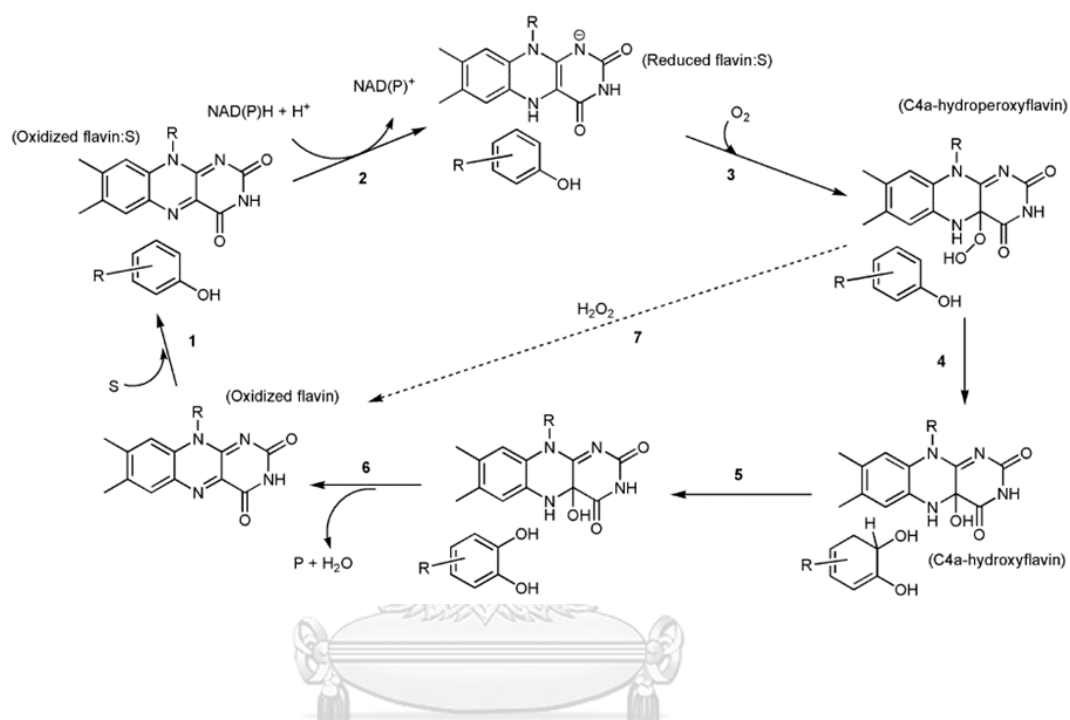
Figure 6: The catalytic cycle of phenolic hydroxylation is carried out by single-component flavin-dependent monooxygenases (hydroxylases).
Taken from: Chenprakhon P, Wongnate T, Chaiyen P. Monooxygenation of aromatic compounds by flavin-dependent monooxygenases. Protein Sci. 2019;28(1):8-29.

The redox reaction of single-component flavin-dependent monooxygenases can be illustrated as follows:

Step 1: Substrate Binding: The aromatic substrate binds to the enzyme, forming an active enzyme-substrate complex.

Step 2: Reductive Half-Reaction: In the presence of the substrate, the reduction of the flavin cofactor (usually FAD) is accelerated by NAD(P)H, acting as a reducing agent.

Step 3: Formation of Hydroperoxyflavin: The reduced enzyme-substrate complex reacts with molecular oxygen, leading to the formation of a C4a-hydroperoxyflavin intermediate.

Step 4: Hydroxylation: The C4a-hydroperoxyflavin intermediate carries out the hydroxylation of the aromatic substrate, resulting in the formation of a hydroxylated product and C4a-hydroxyflavin.

Step 5: Product Release: The hydroxylated product is released from the active site of the enzyme.

Step 6: Flavin Regeneration: The C4a-hydroxyflavin undergoes dehydration, regenerating the oxidized flavin state.

Step 7: In the absence of a substrate or when compounds that bind to the enzyme cannot be hydroxylated, the C4a-hydroperoxyflavin only eliminates H_2O_2, resulting in the formation of oxidized flavin.

This cycle repeats as new substrate molecules bind to the enzyme, facilitating the continuous hydroxylation of phenolic compounds.

A crucial intermediate, known as C4a-hydroperoxyflavin, plays a vital role in all types of flavin-dependent monooxygenases, including both single-component and two-component enzymes. This reactive flavin species acts as an electrophile,

facilitating the insertion of a hydroxyl group into aromatic substrates. In contrast, other flavin-dependent monooxygenases, such as Baeyer-Villiger monooxygenases, employ a distinct reactive flavin species called C4a-peroxyflavin, which acts as a nucleophile (Figure 7). The process of monooxygenation catalyzed by flavin-dependent monooxygenases is involved in diverse biological processes. Single-component flavin-dependent monooxygenases specifically utilize FAD as their cofactor, while two-component monooxygenases employ both FAD and FMN. This distinction in cofactor specificity is likely due to structural motifs that interact with flavins within these enzymes.
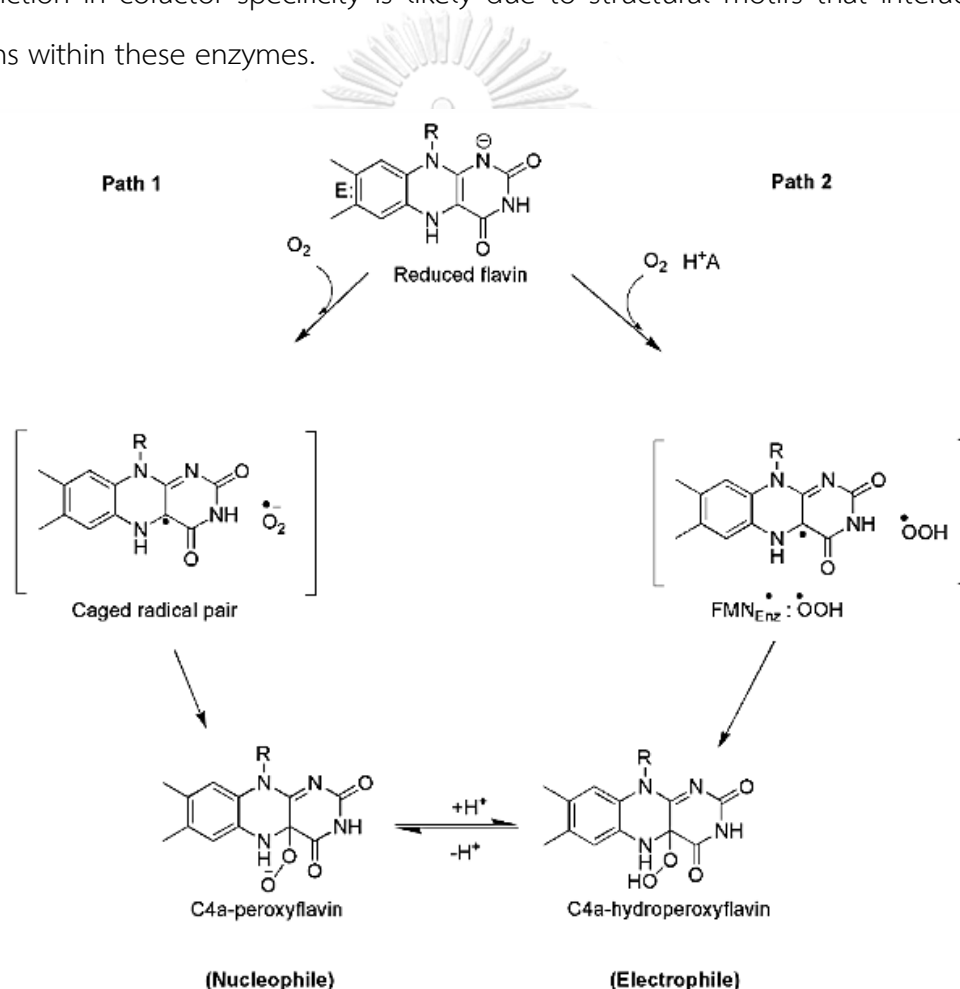
Figure 7. The reaction between reduced flavin and dioxygen, leading to the formation of C4a-(hydro)peroxyflavin, involves an electron transfer from the reduced flavin to oxygen.

This generates a radical pair consisting of flavin semiquinone and oxygen superoxide. Traditionally, Path 1 has been proposed as the model for this reaction in flavin-dependent monooxygenases. In Path 1, only electron transfer occurs in the initial step, followed by the combination of the radical pair to form C4a-peroxyflavin. This intermediate can then undergo further protonation. However, recent investigations using a combination of theoretical chemistry and transient kinetic studies on enzymes such as pyranose 2-oxidase (P_2O) and C2 monooxygenase have revealed a different mechanism. In this alternative mechanism, known as Path 2, the electron transfer step is found to be synchronous with a proton transfer. This process, referred to as proton-coupled electron transfer, leads to the formation of C4a-hydroperoxyflavin. Therefore, the reaction pathway for the formation of C4a-hydroperoxyflavin in flavin-dependent monooxygenases can occur via either Path 1 or Path 2, depending on the specific enzyme and conditions involved. Taken from: Chenprakhon P, Wongnate T, Chaiyen P. Monooxygenation of aromatic compounds by flavin-dependent monooxygenases. Protein Sci. 2019;28(1):8-29.

1.4.2 Two-component flavin-dependent monooxygenases

Flavin reduction in two-component flavin-dependent monooxygenases occurs within the reductase component of the enzyme. These reductases typically bind FAD or FMN as cofactors, although they can also be isolated in an apoenzyme form. They can be directly reduced by NAD(P)H without the need for aromatic compound binding (Step 1 in Figure 8). However, there are exceptions, such as the C1 reductase, where aromatic compounds can bind and enhance flavin reduction. During the oxygenation reaction of two-component enzymes, the enzyme-bound reduced flavin reacts with oxygen to form C4a-hydroperoxyflavin (Step 3 in Figure 8). Two-component enzymes can utilize various types of reduced flavins, including FAD, FMN, and riboflavin, depending on their specific recognition features. The different usage of flavins in two-component monooxygenases is attributed to the flavin binding characteristics.

The presence or absence of aromatic substrates during the oxygenation step depends on the specific requirements of each enzyme. Following the oxygenation step, the reaction of two-component enzymes generally proceeds similarly to that of single-component enzymes. However, there are several distinct features that differentiate these two enzyme types. These include differences in the stability of C4a-hydroperoxyflavin, the order of substrate binding, and the mode of reduced flavin transfer (Step 2 in Figure 8). The transfer of reduced flavin is an essential part of the reaction in two-component monooxygenases but is not required for single-component monooxygenases. These differences contribute to the unique characteristics and mechanisms of two-component monooxygenases (Chenprakhon et al., 2019).
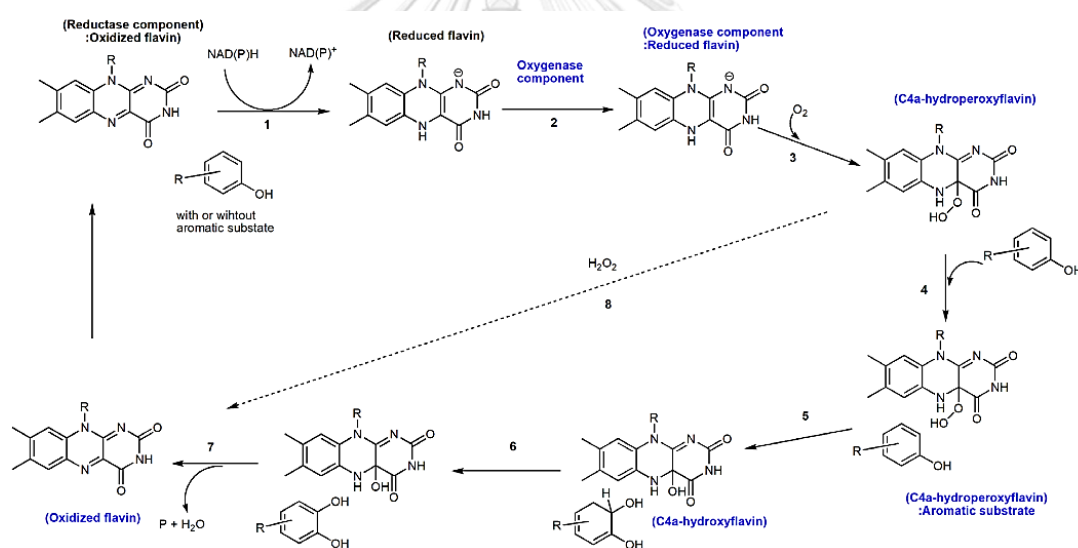
Figure   8. The catalytic cycle of phenolic hydroxylation in two-component flavin-dependent monooxygenases (hydroxylases)

Objectives

1.	To clone the indole monooxygenase gene from *Acinetobacter baumannii* genomic DNA, and subcloned into the expression vector

2.	To produce a high level of recombinant enzymes for mechanistic study

3.	To investigate the kinetics mechanism using rapid kinetics

จุฬาลงกรณ์มหาวิทยาลัย
CHULALONGKORN UNIVERSITY

CHAPTER II

MATERIALS AND METHODS

2.1 Materials

2.1.1 Enzyme, plasmid, genomic DNA, bacteria strain, and marker

Alkaline phosphatase, Quick CIP (BioLabs Inc., England, UK)

Chaperone pGro7 (Takara Bio Inc., Shiga, Japan)

DNA Ladder (SibEnzyme, Siberia, Russia)

ECOS^{TM} *E.coli* DE3 (Yeastern Biotech Co., Ltd. Taipei, Taiwan)

Formate dehydrogenase (ENZMART BIOTECH, Bangkok, Thailand)

Genomic DNA of *Acinetobacter baumannii* (Laboratory of Assoc. Prof. Dr. Ruchanok Tinikul, Bangkok, Thailand)

Prestained Protein marker (ENZMART BIOTECH, Bangkok, Thailand)

pET22b+ plasmid (Merck Millipore, Darmstadt, Germany)

Restriction enzymes *NdeI,* and *XhoI* (BioLabs Inc., England, UK)

T4 ligase (ABclonal Biotechnology Co. Ltd, Montluçon, France)

2.1.2 Chemicals and Reagents

Acetonitrile, C_2H_3N (Quality Reagent Chemical Product, New Zealand)

Acrylamide/Bis solution 30% (ENZMART BIOTECH, Bangkok, Thailand)

Agar powder (HiMedia Laboratories, Dindori, India)

Agarose (Omipur, Massachusetts, USA)

Ampicillin (Bio basic Canada Inc, Markham, Canada)

Ammonium Chloride, NH_4Cl (Quality Reagent Chemical Product, New Zealand)

Ammoniumperoxodisulfate, $N_2H_8S_2O_8$ (Merck Millipore, Darmstadt, Germany)

Arabinose, $C_5H_{10}O_5$ (Tokyo chemical industry, Tokyo, Japan)

Bacteriological peptone (OXOID, Basingstoke, United Kingdom)

Boric acid, H_3BO_3 (Quality Reagent Chemical Product, New Zealand)

β-mercaptone (Merck Millipore, Darmstadt, Germany)

Chloramphenicol (Merck Millipore, Darmstadt, Germany)

D-glucose, $C_6H_{12}O_6$ (Ajax Finechem Pty Ltd, Wollongong, Australia)

Dimethyl sulfoxide, DMSO, C_2H_6OS (Emsure, Darmstadt, Germany)

Dithiothreitol, DTT, $C_4H_{10}O_2S_2$ (Cambridge Isotope Laboratories, Massachusetts, USA)

Disodium phosphate, Na_2HPO_4 (QRëC, Quality Reagent Chemical Product, New Zealand)

Ethyl alcohol, C_2H_6O (Emsure, Darmstadt, Germany)

Ethyl acetate, $C_4H_8O_2$ (Quality Reagent Chemical Product, New Zealand)

Ethidium bromide, $C_{21}H_{20}BrN_3$, (Tokyo chemical industry, Tokyo, Japan)

Ethylene diaminetetra acetic acid, EDTA (Quality Reagent Chemical Product, New Zealand)

Flavin Adenine Dinucleotide, FAD (purity ≥ 95%) (Tokyo chemical industry, Tokyo, Japan)

Flavin mononucleotide, FMN (Tokyo chemical industry, Tokyo, Japan)

Formic acid (98%), CH_2O_2 (Cambridge Isotope Laboratories, Massachusetts, USA)

Glycerol 99.5%, $C_3H_8O_3$ (Quality Reagent Chemical Product, New Zealand)

Glycine, $C_2H_5NO_2$, (Elago Enterprises Pty Ltd., Sydney, Australia)

Glacial acetic acid (Quality Reagent Chemical Product, New Zealand)

Guanidine hydrochloride, $CH_5N_3 \cdot HCl$, (Omipur, Massachusetts, USA)

G-25 Sephadex (GH Healthcare, Uppsala, Sweden)

Hydrochloric acid, HCl (Honeywell International Inc., Charlotte, USA)

Imidazole 99%, $C_3H_4N_2$ (Thermo Fisher Scientific, Massachusetts, USA)

Indole (Tokyo chemical industry, Tokyo, Japan)

Indigo (Sigma-Aldrich Chemie, Steinheim, Germany)

Indirubin (Sigma-Aldrich Chemie, Steinheim, Germany)

IMAC-Sepharose (GH Healthcare, Uppsala, Sweden)

Isopropyl alcohol, C_3H_8O (Honeywell International Inc., Charlotte, USA)

Lactose, $C_{12}H_{22}O_{11}.H_2O$ (Elago Enterprises Pty Ltd., Sydney, Australia)

Magnesium Sulfate, $MgSO_4$ (Quality Reagent Chemical Product, New Zealand)

Methanol (Cambridge Isotope Laboratories, Massachusetts, USA)

Nickle (II) Sulfate Hexahydrate, $NiSO_4.6H_2O$ (Quality Reagent Chemical Product, New Zealand)

Nicotinamide adenine dinucleotide, NAD^+ (Fluka biochemika, St. Louis, USA)

Potassium hydroxide, KOH (Merck Millipore, Darmstadt, Germany)

Potassium Dihydrogen Phosphate, KH_2PO_4 (Quality Reagent Chemical Product, New Zealand)

Potassium bromide, KBr (Quality Reagent Chemical Product, New Zealand)

Sephacryl^{TM} S-200 High Resolution (GE HealthCare Technologies Inc., Chicago, USA)

Sodium chloride, NaCl (Emsure, Darmstadt, Germany)

Sodium hydroxide, NaOH (Merck Millipore, Darmstadt, Germany)

Sodium sulfate, Na_2SO_4 (Quality Reagent Chemical Product, New Zealand)

Sodium hydrosulfite, $Na_2S_2O_4$ (Quality Reagent Chemical Product, New Zealand)

Sodium dodecyl sulfate, SDS, $NaC_{12}H_{25}SO_4$, (Omipur, Massachusetts, USA)

Tetramethylethylenediamine, TEMED (Merck Millipore, Darmstadt, Germany)

Tris base, Hydroxymethyl aminomethane (Omipur, Massachusetts, USA)

Yeast extract (OXOID, Basingstoke, UK)

2-hydroxyindole (Combi-Blocks, San Diego, USA)

3-hydroxyindole (Toronto Research Chemicals Inc., Toronto, Canada)

2-mercapto ethanol, C_2H_6SO, (Merck Millipore, Darmstadt, Germany)

2.1.3 Kits

Phusion High-Fidelity PCR Kit (Thermo Fisher Scientific, Massachusetts, USA)

FavorPrep^{TM} Plasmid Extraction Mini Kit (Favorgen Biotech Corp, Ping Tung, Taiwan)

FavorPrep^{TM} GEL/PCR Purification Mini Kit (Favorgen Biotech Corp, Ping Tung, Taiwan)

2.1.4 Glass wares and plastic wares

Bemis™ Parafilm™ M Laboratory Wrapping Film (Thermo Fisher Scientific, Massachusetts, USA)

Beaker (SCHOTT Singapore Pte. Ltd., New Tech Park, Singapore)

Bottle Assy, PP 500 mL (Beckman colter, California, USA)

Microcentrifuge tube 1.5 mL (Molecular BioProducts, Inc., San Diego, USA)

Pasteur pipettes 3 mL non-sterile (Kartell S.p.a., Noviglio, Italy)

2.1.5 Instruments

Autoclave (Scientific promotion co.,LTD, Phrakhanong, Bangkok)

Balance Precisa XB-220 A (Precisa, Dietikon, Switzerland)

EMD Millipore 5123 Amicon Stirred Cell Model 8200 (Cole-Parmer Instrument Company, Illinois, United States)

Drying oven Memmert (United instrument co.,LTD, Bangkok, Thailand)

Fluorescence spectrophotometer RF-6000 (Shimadzu, Kyoto, Japan)

Fast Performance Liquid Chromatography, FPLC ÄKTA pure 25 M1 (Cytiva, Massachusetts, USA)

Gel electrophoresis Minigel (Hercuvan lab system, Milton Cambridge, UK)

Gel documentation EZ Imager (Bio-Rad, California, USA)

High-performance liquid chromatography, HPLC LC-20AD (Shimadzu, Kyoto, Japan)

Isothermal titration calorimetry, ITC MicroCal PEAQ-ITC (Malvern Panalytical, Worcestershire, UK)

Laminar Scanlaf Mars Biosafety cabinet Class 2 (LaboGene, Bjarkesvej, Denmark)

Magnetic stirrer big squid (IKA Works do Brasil Ltd, Taquara, Brazil)

Microcentrifuge TT-14500 PRO (Hercuvan lab system, Milton Cambridge, UK)

Minishaker MS1 (IKA Works do Brasil Ltd, Taquara, Brazil)

Nanodrop 2000 spectrophotometer (Thermo Fisher Scientific, Massachusetts, USA)

pH meter Orion star A111 (Thermo Fisher Scientific, Massachusetts, USA)

Rapid Quenched Flow RQF-73 (TgK Scientific Limited, England, UK)

Refrigerator Forma 89000 series (Thermo Fisher Scientific, Massachusetts, USA)

Refrigerated centrifuge Allegra™ 64R (Beckman colter, California, USA)

Rotary Evaporator Heidolph - Hei-VAP Core (Heidolph Instruments GmbH & Co., Schwabach, Germany)

Spectrophotometer UV-VIS UV-2550 (Shimadzu, Kyoto, Japan)

SDS PAGE PS300B (Hoefer, Massachusetts, USA)

Spin down (Hercuvan lab system, Milton Cambridge, UK)

Sonicator Vibra-cell Ultrasonic Liquid Processer VCX 750 (Biotechnology Research, Newtown, Connecticut)

Stopped-flow spectrophotometer SF-61DX (TgK Scientific Limited, England, UK)

Shaker Unimax 1010 (Heidolph, Schwabach, Germany)

Thermo cycler T100™ (Bio-Rad, California, USA)

Water bath Hetofrig CB60 and Hetomix TBVS (Lab Chiller Heto inter, Florida, USA)

Water Purification System Cascada II, I (Pall Life Sciences, New York, USA)

2.1.6 Software and database

BioEdit (Manchester Science Parks, Pencroft Way, UK)

Chem Draw Ultra 12.0 (PerkinElmer, Macintosh, and Microsoft Windows, Washington, USA)

KaleidaGraph (Synergy International Systems, Inc., Washington, D.C., USA)

Kinetic Studio (Lower Manhattan, New York City, USA)

2.2 Methods

2.2.1 Amplification of the indole monooxygenase (*iifc*) gene and reductase (*iifd*) gene from *Acinetobacter baumannii*

The PCR condition for the amplification of the *iifc* gene was 30 cycles of denaturation at 98°C for 10 seconds, annealing at 55°C for 1 minute, and extension at 72°C for 10 minutes, using the primer sequence specified in Table 1. The PCR product is gel-purified via a GEL/PCR Purification Mini Kit and follows the manual protocol. The gene of *iifd* was synthesized into expression vector pET-22b+ containing C-terminal histidine tag using restriction sites of *Nde*I and *Xho*I at 5' and 3' end, respectively. The genomic data of the *iifd* gene used for this study can be accessed from the National Library of Medicine in the BioProject, specifically under the accessions CP006768.1. (Parales et al., 1997).

Table 2. The sequencing of primers for the amplification of the *iifc* gene

Primer	Sequence 5' → 3'	Restriction site
Forward	GGAATTC**CATATG**CGCCGTATTGC	*Nde*I
Reverse	CCG**CTCGAG**AGCGACTTTTGC	*Xho*I

*The underlined sequences are restriction sites

2.2.2 Construction of indole monooxygenase expression vector

The amplified gene of *iifc* was introduced into expression vector pET-22b+ containing C-terminal histidine tag using restriction sites of *Nde*I and *Xho*I at 5' and 3' end, respectively. The purified PCR product is digested with *Nde*I and *Xho*I and ligated with *NdeI/Xho*I digested pET22b+ vector. The ligation mixture is transformed into ECOS™ *E. Coli* DE3. (Parales et al., 1997).

2.2.3 Large-scale preparation of recombinant indole monooxygenase (IndOx)

The *E. coli* competent cells were transformed with two plasmids: the recombinant expression vector for IndOx and chaperone plasmid pGro7. The transformed cells containing both recombinant vectors were selected on LB agar containing 20 mg/mL ampicillin (for expression vector) and 20 mg/mL chloramphenicol (for pGro7). A single colony was inoculated into starting culture 50 mL of ZY medium containing the same antibiotics at 37℃ for 16 – 18 hours (overnight). 0.2% of the overnight culture was inoculated into a large-scale auto-induction medium of 1 L in 2.5 L Fernbach flasks (3 flasks). The cultures were incubated in an orbital shaker at 37℃ at the speed of 180 rpm for 3 hours, and then the temperature was decreased to be 20℃ for overnight. Recombinant cells were harvested, and the cell pellet was kept at ー80℃ until used (Grabski et al., 2005).

2.2.4 Large-scale preparation of recombinant reductase (IndR)

The recombinant plasmid of IndR was transferred to *E. coli* competent cells. The transformed cells were selected on LB agar containing 20 mg/mL ampicillin. A single colony of transformed cells was inoculated in the starting culture of 50 mL of ZY medium containing the same antibiotics at 37℃ for 16-18 hours (overnight). For large-scale preparation, 0.2 % of the overnight culture was inoculated into the auto-induction medium of 1 L in 2.5 L Fernbach flask (3 flasks). The culture was incubated in an orbital shaker at 37℃ with the speed of 180 rpm for 3 hours, and the temperature was changed to be 20℃ for overnight. The culture medium was harvested, and the cell pellet was kept at ー80℃ until used (Grabski et al., 2005).

2.2.5 Purification of the indole monooxygenase (IndOx)

The cell pellet of IndOx was thawed and re-suspended in 30 mM imidazole in 50 mM sodium phosphate pH 7.0, 300 mM NaCl. The cell rupture was carried out using an ultrasonic sonicator. The cell lysate was centrifuged at a speed of 18,000 rpm at 4°C for 1 hour to discard cell debris. The supernatant was loaded into the IMAC sepharose column (ϕ 2.5 cm $\times$ 14 cm). The column was charged with 0.2 M nickel sulfate and equilibrated with 30 mM imidazole in 50 mM sodium phosphate pH 7.0, 300 mM NaCl. The column was washed with 500 ml of the same equilibration buffer. The enzyme fraction was eluted with 250 mM imidazole. The eluted enzyme was concentrated using a stirred cell device under a nitrogen-positive pressure (50-70 Psi) with molecular weight cut off 10 kDa to obtain volume $\sim$10 mL. Imidazole in concentrated enzyme was removed using Sephadex G-25 equilibrated with 50 mM sodium phosphate buffer pH 7.0, 300 mM NaCl. The purity of the enzyme was judged on SDS-PAGE. The concentration of IndOx was determined using an extinction coefficient at 280 nm of 73.3×10^3 $M^{-1}cm^{-1}$. (Abdurachim & Ellis, 2006; Han et al., 2013).

2.2.6 Purification of the reductase component (IndR)

The cell pellet of IndR was re-suspended in 50 mM imidazole in 25 mM tris-hydroxymethyl aminomethane pH 7.0, 300 mM NaCl. The cell rupture was performed using an ultrasonic sonicator. The cell lysate was centrifuged at a speed of 18,000 rpm at 4°C for 1 hour. The supernatant was loaded into IMAC Sepharose column (ϕ 2.5 cm $\times$ 14 cm) equilibrated with 30 mM imidazole in 25 mM tris-hydroxymethyl aminomethane buffer pH 7.0, 300 mM NaCl. Unbound proteins are removed with 500 mL of the same buffer used for equilibration. Proteins are eluted with 25 mM tris-hydroxymethyl aminomethane buffer pH 7.0, 300 mM NaCl and 300 mM imidazole after that add 1 mM DTT and FAD until saturating of an enzyme. The eluted enzyme was concentrated using a stirred cell device under a nitrogen-positive pressure (50-70 Psi) with molecular weight cut off 10 kDa to obtain volume $\sim$10 mL.

The imidazole is removed from the concentrated enzyme using Sephadex G-25 equilibrated with 25 mM tris-hydroxymethyl aminomethane buffer pH 7.0. The purity of the enzyme is determined by SDS-PAGE. The concentration of protein is determined using an extinction coefficient at 456 nm of 11.97 $M^{-1}cm^{-1}$. (Abdurachim & Ellis, 2006; Han et al., 2013).

2.2.7 Determination of native molecular weight using fast protein liquid chromatography (FPLC)

The native molecular weight of both the IndOx and IndR were determined using gel filtration. and the reductase were loaded into the gel filtration column of Sephacryl S-200 with high resolution (ϕ 2.5 cm x 73.2 cm in length). The column was equilibrated with 50 mM sodium phosphate buffer pH 7.0 and 300 mM NaCl. The protein standard includes 4 mg/mL aldolase, 0.3 mg/mL ferritin, 3 mg/mL conalbumin, and 10 mg/mL blue dextran. After that load protein all of 2 mM IndOX and 1.81 mM IndR into a column (Madadlou et al., 2011).

Equation 1: Molecular weight determination from the K_{av} values

$$K_{av} = \frac{V_e - V_0}{V_c - V_0} \qquad \text{Equation 1}$$

- K_{av} = partition coefficient

- V_e = elution volume (mL)

- V_o = void volume (mL)

- V_c = geometric column volume (mL)

2.2.8 Activity assay of IndR

The activity assay of IndR was performed using NADH consumption. The reaction was monitored a decrease in absorbance at 340 nm. The concentration of enzymes contains 30 µM IndR with varying concentrations of NADH mixed with 50 mM sodium phosphate buffer pH 7.0 and 300 mM NaCl (Sheng et al., 2001).

2.2.9 Characterization of the native cofactor of the reduced component

The native flavin cofactor and the flavoprotein reductase component (IndR) were subjected to analysis. The enzyme, which had precipitated, was separated from the flavin by utilizing 5% trichloroacetic acid (TCA). Subsequently, the unidentified cofactor was examined using the HPLC LC-20 Series equipment. For detection, a diode-array SPD-20A detector was employed, and a C18 column measuring 4.6 × 250 mm was utilized for separation. The mobile phase consisted of 12% acetonitrile and 1% formic acid in water for equilibration and separation, with a flow rate of 0.5 mL/min. The column temperature was maintained at a constant 25°C. By comparing the retention time with that of authentic flavin molecules such as FAD and FMN, the flavin cofactor was successfully identified (Iwahana et al., 2014).

2.2.10 Oxygen scrubbing the flow system of the stopped flow machine.

The rapid kinetic was performed using a stopped-flow spectrophotometer. All reactions were performed in 50 mM sodium phosphate buffer pH 7.0 and 300 mM NaCl. Oxygen in the flow system of the instrument was eliminated using sodium bisulfite (5 mg/mL). The anaerobic sodium bisulfite was prepared in a closed container tonometer. The buffer in the tonometer was made anaerobic using ultrapure high purity (UHP) of nitrogen gas (purity ≥ 99.99%) through an anaerobic train. Anaerobic condition was made by connecting tonometer with two-way oblique manifold for alternating between equilibrating buffer under positive pressure of nitrogen gas and evacuation for forty cycles through. The tonometer was connected to an anaerobic train with of alternating and positive pressure of connecting through a three-way oblique stop cock. Then the sodium bisulfite powder in the side arm

was mixed with an anaerobic buffer. The anaerobic solution of sodium bisulfite was transferred from the tonometer to the flow system of the stopped-flow machine and left overnight. The flow system was washed with an anaerobic buffer three times. The anaerobic buffer or substrate solution was prepared by equilibrating the buffer with UHP nitrogen gas with bubbling the buffer in 10 mL glass syringe *via* long needle connected to anaerobic train for 6 mins (Sucharitakul et al., 2021).

2.2.11 Rapid kinetics reduction of IndR component

The kinetic reduction of the reductase component was performed by mixing an anaerobic solution of the oxidized enzyme with an anaerobic solution of NADH. The concentrations of NADH were varied under pseudo-first order condition using NADH over enzyme concentration at least 5-fold. The oxidized enzyme was made anaerobic in a tonometer using an anaerobic train for evacuation and equilibration of UHP nitrogen gas as described above. The anaerobic enzyme solution was transferred from the tonometer to the drive syringe of the stopped-flow machine. The transfer of anaerobic enzyme solution in tonometer was controlled by three-way oblique stop cock through the glass luer tip fitted to the holder of stopped-flow machine without exposure to air. The varied NADH concentrations were made anaerobic by bubbling in glass syringe with UHP nitrogen gas (from anaerobic train) *via* a long needle syringe and then transferred to the drive syringe of the stopped-flow machine. The anaerobic enzyme solution and varied NADH concentrations were mixed in the stopped-flow machine. The reactions were monitored using absorbance in the range of 350 – 700 nm for flavin semiquinone, flavin reduction, and charge-transfer complex (Sheng et al., 2001).

2.2.12 Rapid kinetics oxidation of IndOx component

Rapid kinetic study of oxidative reaction was performed using either free reduced FAD or reduced FAD in complex reacting with oxygenated buffer. The solution of free FAD or its complex with the monooxygenase was made anaerobic in a tonometer using the same procedure as previously described. Dithionite solution

(reductant) of 5 mg/mL was made anaerobic using bubbling of nitrogen gas with a long needle in a glass syringe (for 6 mins). The micro-titrator with a long needle was filled with anaerobic dithionite solution, and the micro-titrator was attached to the tonometer via a Michael-Miller adaptor under positive nitrogen pressure. Dithionite solution was put into the solution in a tonometer by turning the knob of the micro-titrator. The stoichiometric reduction of the enzyme-bound FAD was monitored by flipping the solution into a side arm attached to a quartz cuvette to observe the changing spectra of oxidized to fully reduced flavin without excess dithionite. The spectral change from flavin reduction was monitored using the spectrophotometer with a diode array detector. The anaerobic reduced enzyme solution was transferred from a tonometer to a drive syringe of the stopped-flow machine. The varied oxygen concentrations were prepared by bubbling with different percentages of O_2/N_2 of 50% and 100% *via* a long needle syringe and then transferred to a drive syringe of the stopped-flow machine. Both reduced enzyme and varied oxygen concentration buffers were mixed in the stopped-flow machine. The reactions were monitored using absorbance in the range of 350 – 700 nm for flavin semiquinone and flavin oxidation (Sucharitakul et al., 2021).

2.2.13 Analysis of kinetic mechanisms

The kinetic traces obtained from a change in optical properties: absorption or fluorescence, were analyzed to determine the observed rate constant (k_{obs}) through exponential fitting using the software package Kinetic Studio version 5.1.0.6 (TgK Scientific, UK). The observed rate constants were plotted against substrate concentrations under pseudo-first order condition to analyze the pattern of the plot to interpret the reaction mechanisms. The kinetic parameters such as the rate constants of the elementary steps and dissociation constants (K_d) were obtained using Marquardt–Levenberg nonlinear fitting algorithms included in KaleidaGraph (Synergy Software) (Sucharitakul et al., 2021).

2.2.14 Determination of the dissociation constant (K_d) for binding of IndOx to reduced FAD (FADH⁻)

The binding of IndOx to reduced FAD to from the complex was determined from an increase in absorbance at 380 nm of C4a-hydroxperoxyflavin intermediate. The complex of IndOx-FADH⁻ reacts with oxygen to form the intermediate whereas the free FADH⁻ is oxidized without forming of the intermediate. The reduced FAD was prepared in tonometer under anaerobic condition as described in (2.2.11) using sodium bisulfite. The FADH⁻ was mixed with varied IndOx concentrations in air-saturation buffer. The reactions were monitored an absorbance change at 380 nm. An increase in absorbance at 380 nm (ΔA_{380}) was referred to amount of the IndOx-FADH⁻ complex. The value of ΔA_{380} was determined from the kinetic trace of absorbance at time of 0.05 s using the kinetic trace from mixing of free FADH⁻ with air-saturation buffer as reference value. The hyperbolic curve of a plot of ΔA_{380} versus IndOx concentrations was used to determine the K_d for IndOx-FADH⁻ complex according to Equation 2. (Sucharitakul et al., 2021).

$$ ES = \frac{(E_0 + L_0 + K_d) \pm \sqrt{(E_0 + L_0 + K_d)^2 - 4E_0L_0}}{2} \qquad \text{Equation 2}$$

- ES = the substrate is attached to a defined place on the enzyme.
- E_o = concentration of enzyme (μM)
- L_0 = concentration of FAD (μM)
- K_d = the equilibrium dissociation constant

2.2.15 Determination of K_d for binding of oxidized FAD to IndOx and K_d for binding of IndOx-FAD complex to indole

The binding of FAD to indole was performed by titration of 10 μM FAD with varied IndOx concentrations. The binding to form the complex was monitored an increase in emission intensity of FAD with excitation at 450 nm. The emission spectra

(470 - 700 nm) from each varied concentration of IndOx were collected. The different values (ΔF) of emission intensity at 532 nm from titration using the emission intensity of free FAD at the same wavelength as reference value were calculated. The value of ΔF_{max} was referred to 10 μM of IndOx-FAD complex (ES) and used to calculate [ES] at varied IndOx concentrations. The K_d value was determined from a plot of [ES] *versus* IndOx concentrations. The valuable biomolecular interactions characterize the binding properties of oxidized FAD using Equation 2. The reactions were performed in 50 mM potassium phosphate buffer pH 7.0, 300 mM NaCl (Sucharitakul et al., 2021).

The binding of IndOx-FAD complex to indole forming a ternary complex was performed using 10 μM FAD in saturation with IndOx. The concentration of IndOx was greater than > FAD with 5-fold of K_d of IndOx-FAD complex. The enzyme complex was titrated with varied indole concentrations. The binding to form ternary complex was monitored a decrease in emission intensity of IndOx-FAD complex with excitation at 450 nm. The K_d for ternary complex was analyzed as the same procedure as described above.

2.2.16 Analysis of 3-hydroxtindole using high-performance liquid chromatography (HPLC)

2.2.16.1 Identification product using single turnover reactions

A reaction mixture was created by combining 150 µM IndOx and 1 mM indole in 50 mM potassium phosphate containing 10% DMSO, and 300 mM NaCl pH 7.0. The 30 µM FAD was made anaerobic in the tonometer under positive nitrogen. All concentrations were after mixing concentration. The solution of FAD was stoichiometrically reduced using sodium bisulfite. An anaerobic FAD was reduced using microtitrator with a long needle connected to a Michael-Miller adaptor. The reductive titration was monitored as a decrease in absorption spectra of flavin bound enzyme with a diode array detector. The tonometer was opened and an equal volume of air-saturation buffer containing IndOx was added to start the catalytic

reaction. The reaction was left for 10 sec. The reaction mixture was quenched using a 0.075 M HCl. After quenching, 25 mM DTT was added to protect an oxidation of the 3-hydroxyindole product by atmospheric oxygen before HPLC analysis (Céspedes et al., 2009).

2.2.16.2 Identification product using multiple turnover reactions

The multiple turnover reaction contained 1 mM NAD^+, 50 mM formic acid, 0.0198 unit formate dehydrogenase, 5 mM indole, 150 µM IndOx, and 30 µM IndR. The reaction was performed in 50 mM potassium phosphate, and 300 mM NaCl pH 7.0 with total volume of 5 mL. The reaction was incubated at room temperature air-saturation overnight (∼16 h.). 3-hydroxtindole and indigo were extracted from the solution. 2 mL of 100% DMSO was added to the reaction 5 mL until it became homogeneous. Subsequently, 10 mL of ethyl acetate was added, and the extraction process was repeated three times. The ethyl acetate fraction was then evaporated to remove any remaining ethyl acetate. The resulting residue was dissolved in 100% DMSO, filtered, and subjected to analysis by HPLC (Céspedes et al., 2009).

3-hydroxyindole and indigo were analyzed using HPLC. The compounds were separated using C18 reversed-phase column (4.6 ϕ cm x 250 mm). The column was equilibrated with 30% methanol in H_2O with a flow rate of 0.5 mL/min. The separation was performed in the oven at 35°C. The 3-hydroxyindole and indigo were monitored an absorbance at 378 nm and 610 nm, respectively. The concentrations of 3-hydroxtindole were determined using the calibration curve of the peak area of the chromatogram of the authentic compound. The binary gradient mode for mobile phase was described in Table 3. (Pimviriyakul et al., 2018).

Table 3. The binary gradient profile involves increasing the percentage of methanol in the mobile phase from an initial value to a final value over a specified time period

| Time	% Methanol (volume)
10	30
20	40
30	60
40	80
50	100
60	100
65	80
70	60
80	30

2.2.17 Analysis of the rate constant for hydroxylation of indole using rapid quenched flow

The 30 Equation 2 µM FADH$^-$ was prepared in an anaerobic glove box. The FAD solution was stoichiometrically reduced using anaerobic sodium bisulfite solution (5 mg/mL). The FADH$^-$ was mixed with 150 µM IndOx containing 1 mM indole in air-saturation. The reactions were quenched with 0.075 M HCl at different times of 0.004, 0.008, 0.02, 0.04, 0.08, 0.1, 0.2, and 0.4 s using the rapid-quenched flow machine. The quenched solutions were kept and added 25 mM DTT to prevent oxidation of the 3-hydroxyindole product by atmospheric oxygen before HPLC analysis. The solutions were centrifuged to discard precipitated protein. The soluble protein was separated using membrane filter cut off 10 kDa. C18 reversed-phase column (4.6 ϕ cm x 250 mm) was equilibrated with 50% methanol in water with flow rate of 0.5 mL/min. The separation was performed in oven at 35℃. The concentrations of 3-hydroxtindole were determined using the calibration curve of the

peak area of the chromatogram of the authentic compound. The rate constant for hydroxylation was determined from a plot of 3-hydroxyindole concentrations *versus* time using Marquardt–Levenberg nonlinear fitting algorithms included in Kaleida Graph (Synergy Software) (Pimviriyakul et al., 2018).

2.2.18 Investigation of the binding of isothermal titration calorimetry (ITC)

The binding of the oxygenase component to indole was investigated using ITC. The reaction was performed using 150 µM IndOx, and 1 mM indole in 50 mM potassium phosphate buffer containing 300 mM NaCl, and pH 7.0. The IndOx was loaded into the sample cell, reference cell was loaded water, and indole was loaded into syringe injection. The experiments were performed under stir speed of 750 rpm at 25°C. The injection volume was 3 µL of indole with total times of 13. (Johnson, 2021).
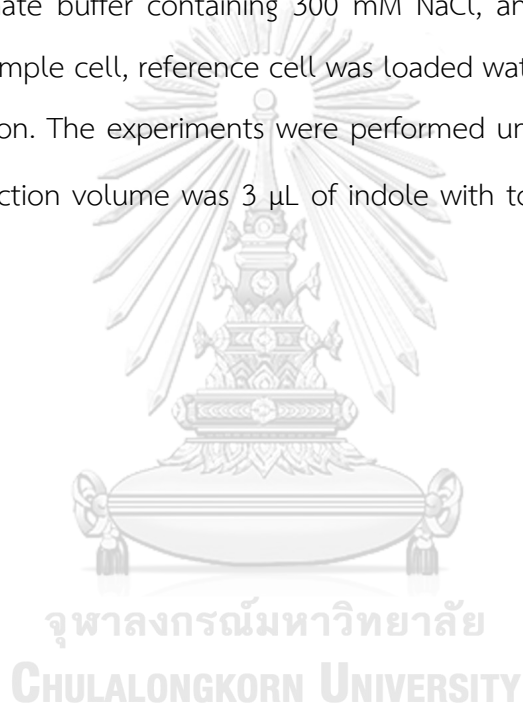
CHAPTER III

RESULTS

3.1 Construction of the expression vector for IndOx

The primers containing *Nde*I and *Xho*I restriction sites at 5' and 3', respectively, were used for amplification *iifc* gene of *Acinetobacter baumannii* sp. for IndOx using genomic DNA as a template. The expected size of amplified *iifc* gene was 1.2 kb (Lane 1, Figure 9A). The amplified IndOx gene was cloned into the pET22b+ using *Nde*I and *Xho*I restriction sites. The clones of bacteria containing the recombinant plasmid were screened using double digestion to detect the *iifc* gene with the size of 1.2 kb (Figure 9B).
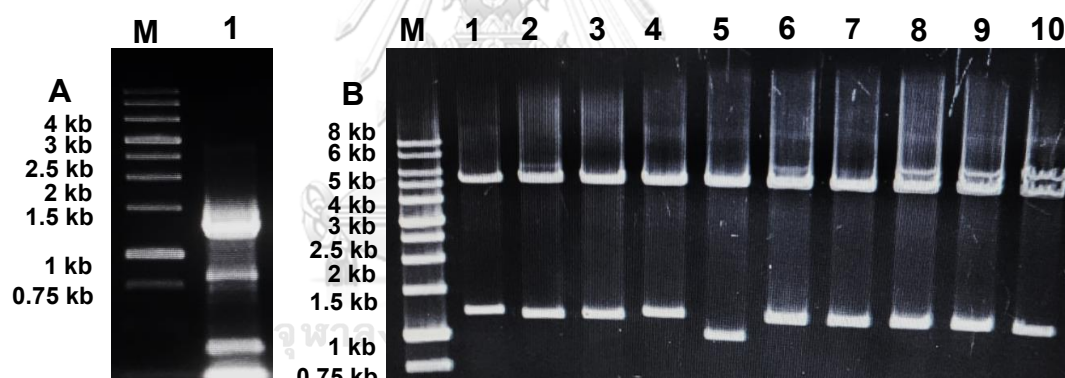

Figure 9. Amplification of *iifc* gene from genomic DNA and construction of an expression vector for IndOx.

The DNA samples were run in 1% agarose gel using TE buffer. The band of DNA was detected using ethidium bromide under UV light. **A)** The amplified *iifc* gene in a gel. Lane M: DNA markers, lane 1: the amplified *iifc* gene. **B)** Screening of the recombinant plasmid. Lane M: DNA markers, lanes 1 to 10 were selected recombinant plasmids for screening of *iifc* gene with expected size of 1.2 kb using restriction enzymes for double digestion.

3.2 Enzyme characterization

Recombinant plasmid of indole monooxygenase (IndOx) was cloned, and reductase component (IndR) was synthesized from company, with C-terminal histidine tags, were expressed in *E. coli* as soluble proteins. The yields of pure proteins were approximately 0.31 g/L and 0.11 g/L of cell culture for IndOx and IndR, respectively. The purity of the enzymes was assessed using SDS-PAGE in Figure 10. The IndOx protein demonstrated a high yield and an expected size of 47 kDa, while the IndR protein had a size of 19 kDa. The purity of IndOx was 97.8% and IndR was 94.8%.
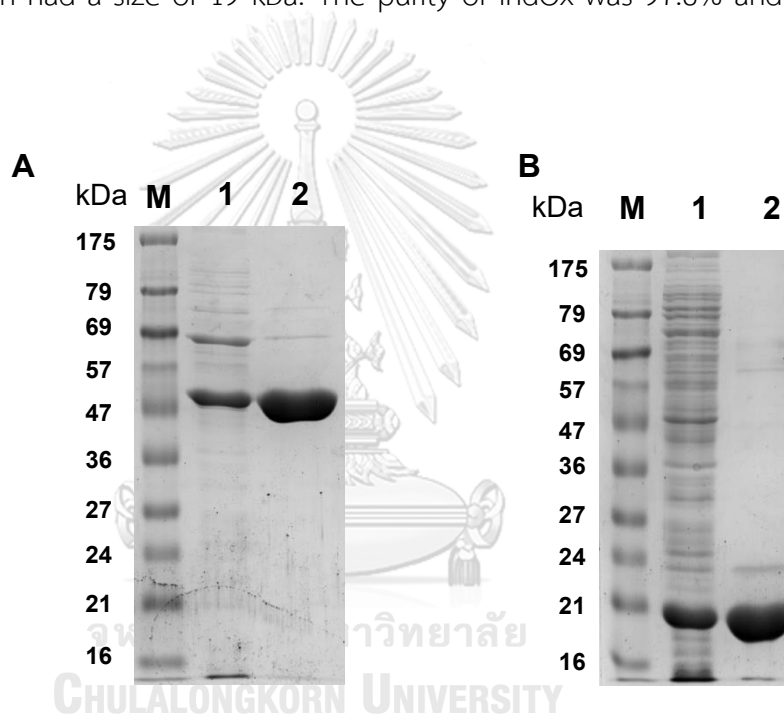

Figure 10. Separating and analyzing proteins on 12% SDS-PAGE.
A) Purification of IndOx. Lane M: protein markers, Lane 1: crude cell lysate, and Lane 2: the elution fraction of IndOx with expected of 47 kDa. **B**) Purification of IndR. Lane M: protein markers, Lane 1: crude cell lysate, and Lane 2: the elution fraction was expected to be 19 kDa.

3.3 Analysis of the native cofactor of IndR using HPLC

The absorption spectrum of the IndR showed peak at 350 and 450 nm wavelengths, which was a characteristic of flavin (Figure 11A). The pure reaction of IndR yellow color of enzyme-bound oxidized flavin. To identify the native cofactor, the enzyme was precipitated using 5% trichloroacetic acid. The released flavin was identified using HPLC. Standard compounds of FAD and FMN were used to identify the native flavin from denatured proteins. The HPLC chromatogram showed peak of standard FAD and FMN at 12.8 and 17.7 min, respectively (red line, Figure 11B). The isolated flavin cofactor from IndR exhibited the same peak of FAD at 12.8 min (blue line, Figure 11B). The determination of the flavin content in IndR using 5% TCA revealed it to be 99.09% FAD.
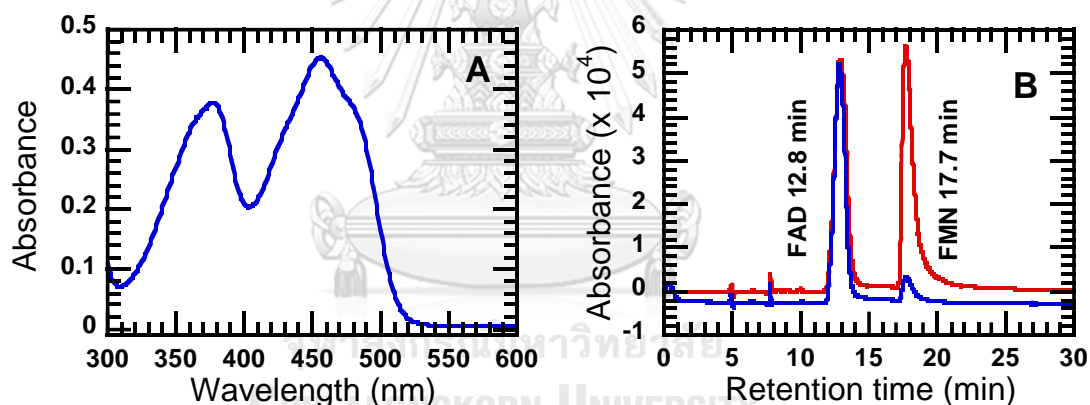

Figure 11. Identification of the native cofactor of IndR.

A) The flavin-bound IndR spectrum. **B**) The separation peak of FAD and FMN using HPLC (red line). The isolated native flavin from IndR was separated of which the type of flavin bound IndR was FAD (blue line).

3.4 Determination of native molecular weight using fast protein liquid chromatography (FPLC)

The standard molecular weight proteins were loaded in the gel filtration Sephacyl S-200. The elution fraction of each protein was monitored absorbance at 280 nm (Figure 12A). The chromatogram of peaks of standard molecular weight were ferritin (440 kDa), aldolase (158 kDa), conalbumin (75 kDa), and ovalbumin (43 kDa), respectively. A plot of partition coefficients of each standard proteins *versus* log (MW) showed linear correlation (Figure 12B). According to the calibration curve, the estimated size of IndOx from FPLC was 93.7 kDa whereas the size based amino acid sequence was 47 kDa. The result indicated that IndOx was in dimer. For the IndR, the estimated size from FPLC was 25.5 kDa whereas the size calculated from amino acid sequence was 19 kDa. The IndR didn't confirm from this standard curve.
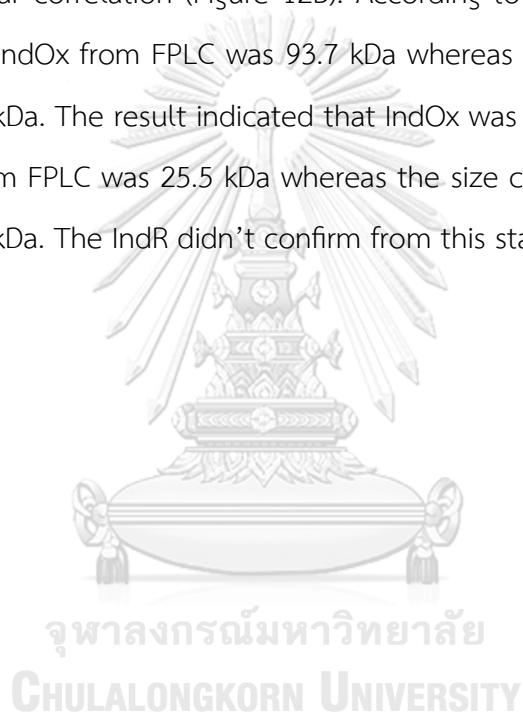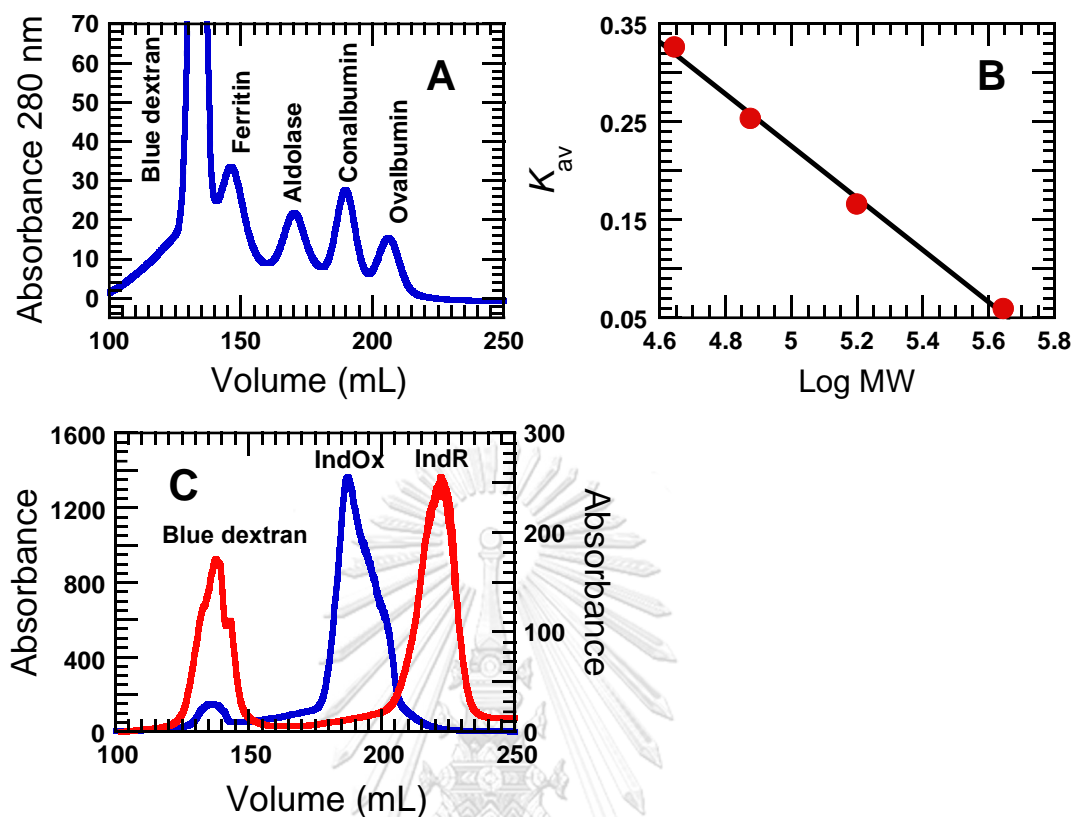
Figure 12. Determination native form of IndOx and IndR.

A) The chromatogram of standard protein molecular weights. The linear equation of the calibration curve incorporates four proteins: ferritin, aldolase, conalbumin, and ovalbumin, along with blue dextran. **B**) The calibration curve of a plot partition coefficient (K_{av}) of protein molecular weights versus log MW. A) Chromatography is utilized to determine the molecular weight and size of proteins. Blue dextran is the first high molecular weight glucose polymer to be eluted from the column, followed by ferritin, aldolase, conalbumin, and ovalbumin, respectively. **C**) The chromatogram of IndOx and IndR used for determination of the protein molecular weight.

3.5 Analysis of monooxygenation product of IndOx using HPLC

HPLC was used for the separation of the product from the reaction components with identification of the specificity of the hydroxylation position of indole ring. The peaks of standard compounds of indole at 44 min (black line, Figure 13A), 3-hydroxyindole at 24.8 min (blue line, Figure 13A), 2-hydroxyindole at 29 min (green line, Figure 13A) and indigo at 53.6 min (pink line, Figure 13A). It has been known that 3-hydroxyindole can be oxidized by atmospheric oxygen to be a dimer which is indigo in blue color (Han et al., 2012). The HPLC analysis showed an effect of atmospheric oxygen oxidizing 3-hydroxyindole to indigo. The chromatogram in (Figure 13B the red line) was from 3-hydroxyindole exposed to air. There was no peak of 3-hydroxyindole whereas 25 mM dithionite was added to the same solution of 3-hydroxyindole, the peak of 3-hydroxyindole was detected at 24.8 mins (blue line, Figure13B).

The single turnover reaction using 30 μM FADH$^-$ resulted in the production of a single product, namely 3-hydroxyindole. This product was confirmed through high-performance liquid chromatography (HPLC) analysis, which showed a peak at a retention time of 24.8 minutes (Figure 13C), matching the retention time of an authentic compound.

Subsequently, it was determined that the enzyme was capable of exclusively producing 3-hydroxyindole, and the dimerization of 3-hydroxyindole was tested using a multiple turnover reaction. The resulting metabolite was identified as 100% indigo, observed at a retention time of 53.6 min, with no detectable residual 3-hydroxyindole at a retention time of 24.8 min in Figure 13D.
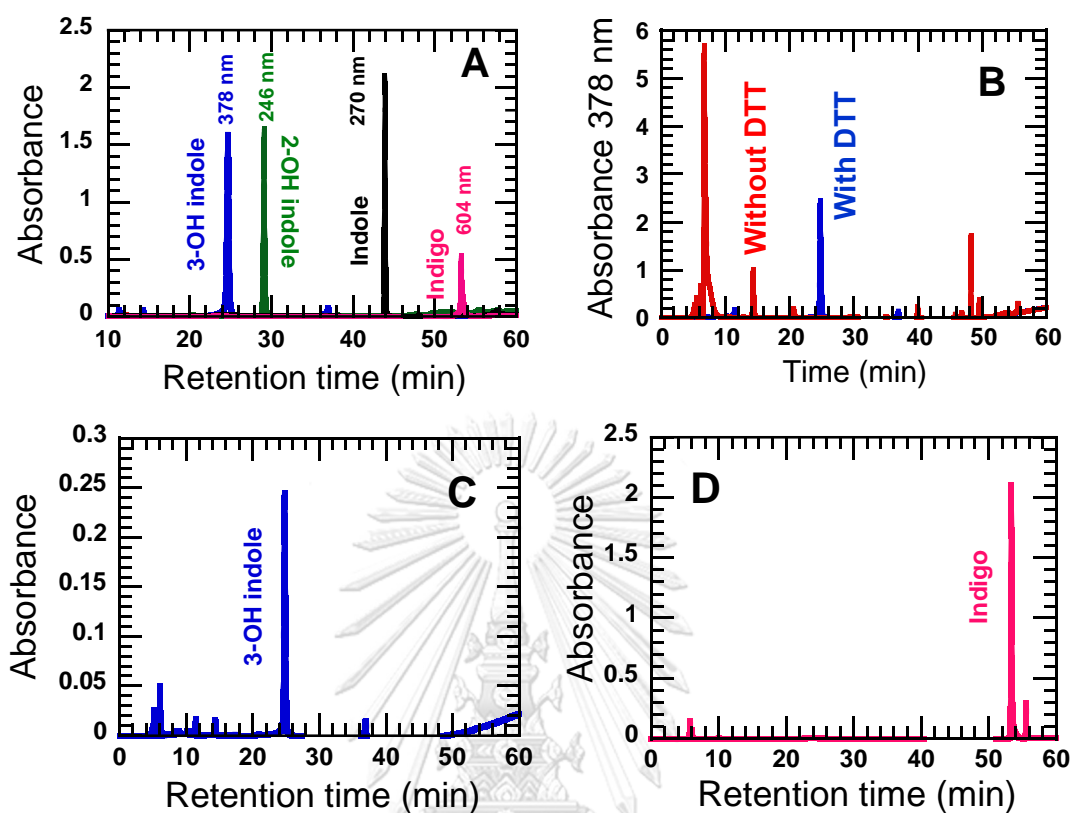
Figure 13. Analysis product from IndOx using HPLC.

A) The chromatogram separation of the authentic compounds. B) Effect of DTT on stability of 3-hydroxyindole. Red line: 3-hydroxyindole without adding DTT resulting in disappearance of 3-hydroxyindole. Blue line: 3-hydroxyindole mixed with DTT. C) The chromatogram of 3-hydroxyindole mixed with DTT and peak of 3-hydroxyindole at 24.8 min. D) The chromatogram of indigo from multiple turnover reaction and peak at 53.6 min.

3.6 Kinetic oxidation of IndOx in complex with reduced FAD (FADH⁻)

The solution of 30 µM FADH⁻ was mixed with 150 µM IndOx in air-saturation buffer. The reaction was monitored for an absorbance change from 300 nm to 600 nm with 5 nm of interval. The maximum absorbance change at 390 nm was monitored for C4a-hydroperoxy flavin whereas the wavelength at 448 nm was monitored for flavin oxidation. The kinetic trace of absorbance change at 390 showed an increase in absorbance of the C4a-hydroperoxyflavin formation (red line, Figure 14A). In contrast, the premixed the same concentrations of solution of FADH⁻ and IndOx showed much less magnitude of absorbance change indicating that the pre-complexed FADH⁻ with IndOx inhibited the C4a-hydroperoxyflavin forming (green line, Figure 14A).

The solution of 30 µM FADH⁻ was mixed with 150 µM IndOx in 0.13, 0.31, and 0.61 mM oxygen concentrations. The kinetic traces at 390 nm showed an increase in absorbance of C4a-hydroperoxyflavin were linearly dependent on oxygen concentrations. The intermediate was stable until 50 s and decayed. The decay of the intermediate was consistent with an increase in absorbance at 448 nm for flavin oxidation with a release of H_2O_2.

A plot of observed rate constants (k_{obs}) for formation of C4a-hydroperoxyflavin versus oxygen concentration resulting in the slope of 3.95 $\pm$ 0.4 $\times$ 10^5 $M^{-1}s^{-1}$ (k) according to Equation 3. The kinetic analysis of the decay C4a-hydroperoxyflavin or flavin oxidation showed the rate constant of 0.0069 $\pm$ 0.0001 s^{-1} Figure 14C.

$$k_{obs} = k[O_2] \qquad \text{Equation 3}$$

- k_{obs} = the observed rate constant

The spectrum C4a-hydroperoxyflavin was deconvoluted using charge couple device (CCD) detector to obtain all absorption spectra from mixing reduced FAD with IndOx in 50% oxygen buffer. The reduced FAD (black line) reacted with IndOx in 50% oxygen buffer to form C4a-hydroperoxyflavin (dotted-red line) with a peak at 380 nm and then the intermediate decayed to be oxidized flavin (blue line, Figure 14B).
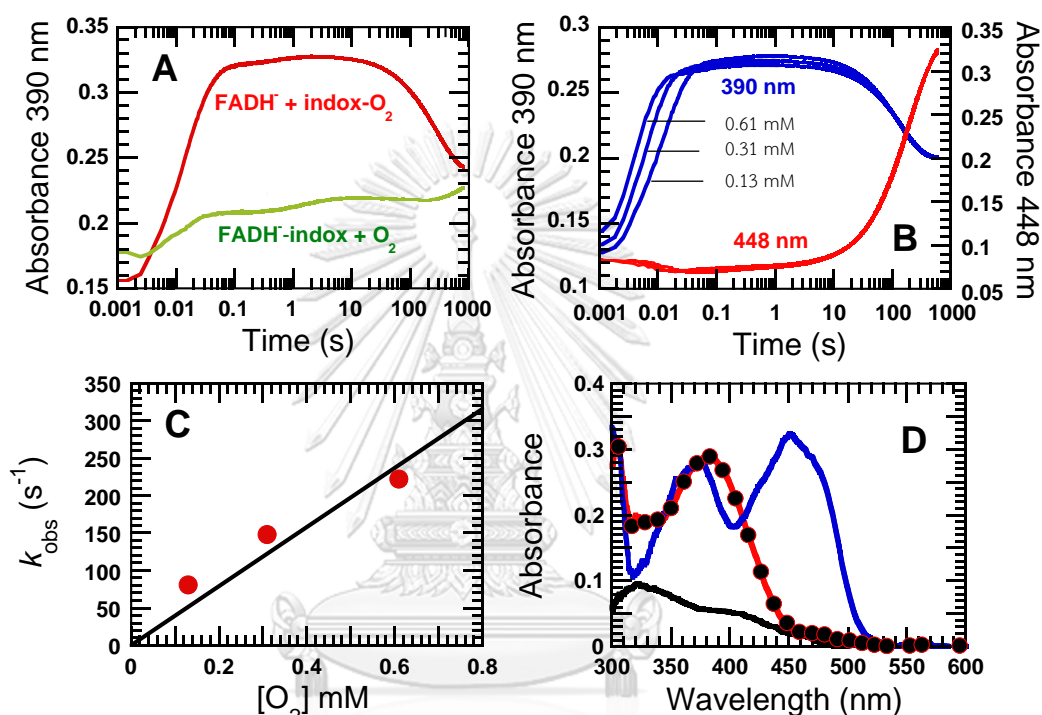

Figure 14. The oxidation FAD¯ in presence of IndOx.

A) Red line: 30 µM FADH¯ was mixed with 150 µM IndOx in air-saturation buffer in stopped-flow spectrophotometer. The reaction was monitored an absorbance change at 390 nm for C4a-hydroperoxyflavin. Green line: the same concentrations of FADH¯ and IndOx were pre-equilibrated. The complex was mixed with an air-saturation buffer. The reaction was monitored at 390 nm. **B**) 30 µM FADH¯ was mixed with 150 µM IndOx in different oxygen concentrations: 0.13 mM, 0.31 mM, and 0.61 mM (from right to left). The reaction was monitored at 390 nm for C4a-hydroperoxyflavin and 448 nm (blue lines) for flavin oxidation (red lines). **C**) A plot of observed rate constants for C4a-hydroperoxyflavin formation versus different oxygen

concentrations. **D**) The absorption spectra from 30 µM FADH⁻ was mixed with 150 µM IndOx in 0.62 mM oxygen buffer. The reaction was monitored using CCD detector. The reduced FAD (black line,) in presence of IndOx was oxidized to form C4a-hydroperoxyflavin intermediate (dotted-red line) and then decayed to oxidized flavin (blue line).

The spectrum of C4a-hydroperoxyflavin intermediate from the same reaction as described in A (closed-circle red line, Figure 14D). The reaction was detected using a charge-coupled device of which spectra were from reduced flavin (black line, Figure 14D) reacting with monooxygenase and oxygen to be oxidized form (blue line, Figure 14D). The reaction mechanism for FADH⁻-IndOx complex is according to Figure 15.
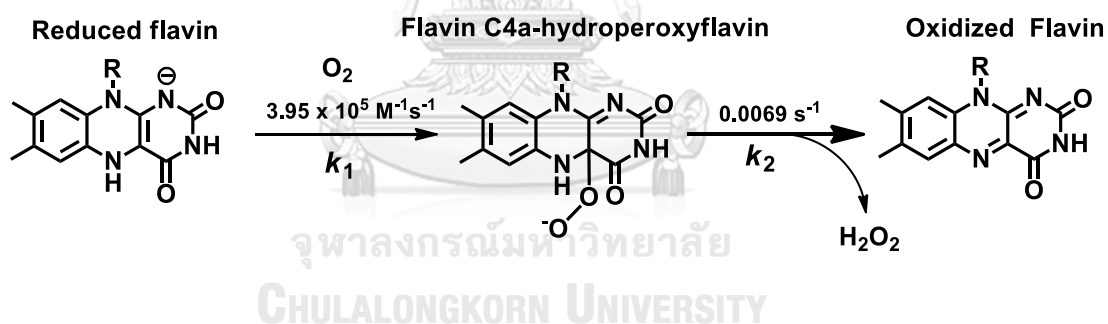

Figure 15. The reaction mechanism of oxidation of FADH⁻ in presence of IndOx.

3.7 Determination of K_d for FADH⁻-IndOx complex

The K_d binding for reduced FAD with IndOx was investigated using C4a-hydroperoxy formation. An increase in absorbance at 390 nm was according to amount of FADH⁻-IndOx complex. The experiments were performed by mixing of reduced FAD with varied IndOx concentrations. The dotted-line showed the control reaction from mixing reduced FAD with air-saturation buffer. The solid lines showed an increase in absorbance at 380 nm at 0.03 s of C4a-hydroperoxyflavin according to an increase in IndOx concentrations (Figure 16A). The different values of absorbance change at 0.03 s were used to calculate concentration of FADH⁻-IndOx complex ([ES]) with K_d of 9.27 ± 1.7 μM in Figure 16B.
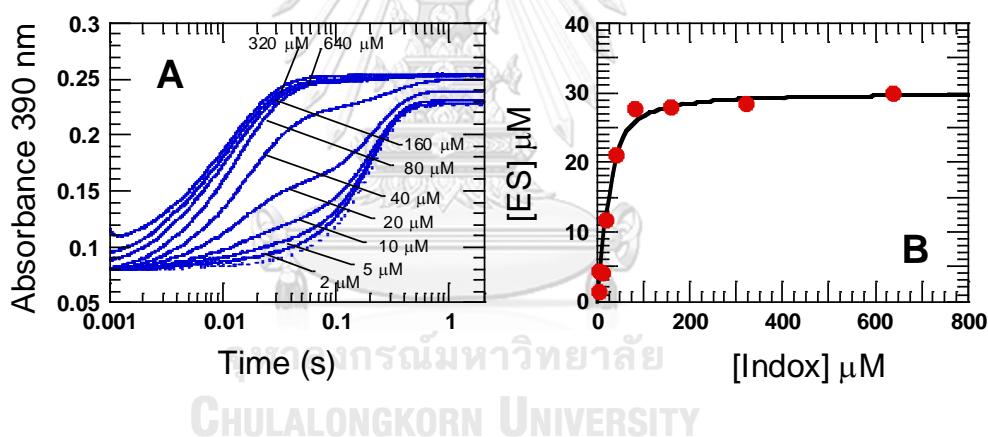
Figure 16. The binding of reduced FAD to IndOx.

A) 30 μM FAD was mixed with 2, 5, 10, 20, 40, 80, 160, 320, 640 μM of IndOx. The reaction was monitored at 390 nm for C4a-hydroperoxyflavin. The kinetic traces at 390 nm showed an increase in absorbance at 390 nm which was referred to the FADH⁻-IndOx complex as shown in solid line. The dotted line was from oxidation of FADH⁻ without IndOx. **B**) Absorbance change at 0.03 s was used to calculate the concentrations of FADH⁻-IndOx complex ([ES]). The K_d value was determined from a plot of [ES] versus IndOx concentrations.

3.8 Kinetic oxidation of IndOx in complex with FADH⁻ in presence of indole

The mixing of reduced FAD with IndOx plus 1 mM indole in air-saturation buffer also showed C4a-hydroperoxy formation at 380 nm (red line, Figure 17A). The observed rate constant for formation of C4a hydroperoxyflavin was the same as FADH⁻-IndOx complex oxidation by oxygen without indole (blue line, Figure 17A). However, the decay of the intermediate in presence was much faster than free enzyme. The C4a-hydroperoxyflavin formation was also dependent on oxygen concentrations (red line, Figure 17B) whereas the decay of the intermediate was also consistent with an increase in absorbance at 448 nm for flavin oxidation (green line, Figure 17B).

A plot of observed rate constants (k_{obs}) for formation of C4a-hydroperoxyflavin versus oxygen concentration resulting in the slope of 2.52 ± 0.2 × 10^5 $M^{-1}s^{-1}$ (k) according to Equation 3. The kinetic analysis of the decay C4a-hydroperoxyflavin or flavin oxidation showed the rate constant of 5.24 ± 0.003 s^{-1} in Figure 17C.
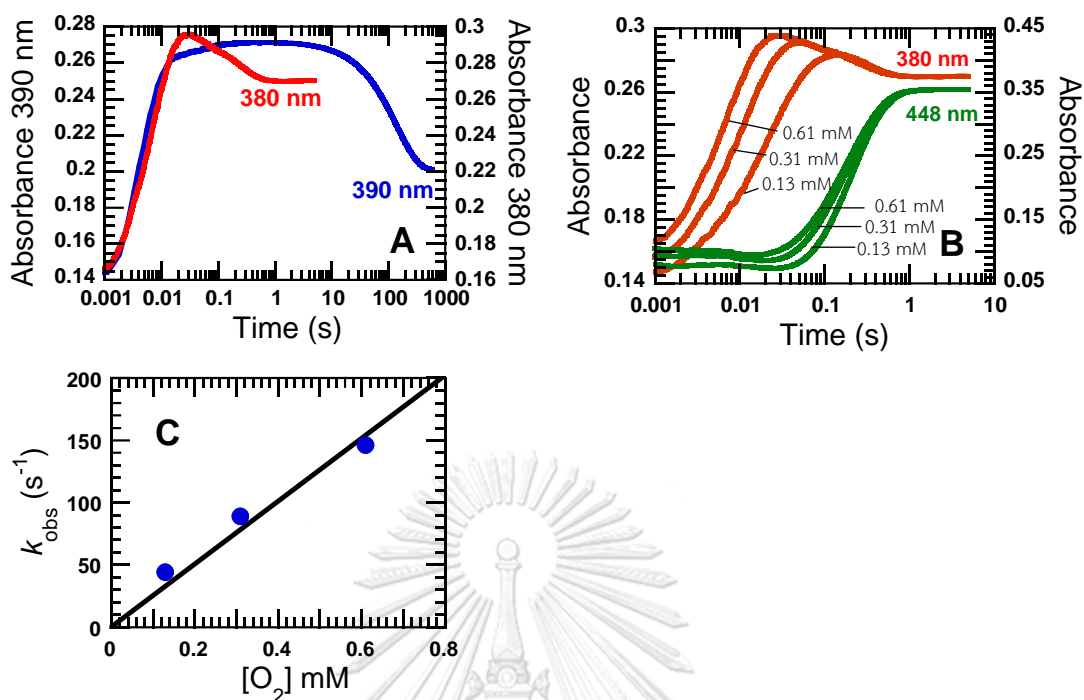
Figure 17. The oxidation FAD⁻ in presence of IndOx and indole

A) 30 µM FAD was mixed with IndOx plus 1 mM indole in air-saturation buffer (red line). 30 µM FAD was mixed with IndOx without indole in air-saturation buffer (blue line). The reactions were monitored at 390 nm for C4a-hydroperoxyflavin. **B**) 30 µM FADH⁻ was mixed with 150 µM IndOx plus 1 mM indole in different oxygen concentrations: 0.13 mM, 0.31 mM, and 0.61 mM (from right to left). The reaction was monitored at 390 nm for C4a-hydroperoxyflavin and 448 nm (red lines) for flavin oxidation (green lines). **C**) A plot of observed rate constants (k_{obs}) for C4a-hydroperoxyflavin formation versus different oxygen concentrations.

3.9 Hydroxylation of indole

It has been known that some flavoprotein hydroxylases have fluorescence properties of C4a-hydroxyflavin intermediate after hydroxylation. In this experiment, the fluorescence mode of stopped-flow spectrophotometer was applied. The mixing of FADH⁻ with IndOx in 50% oxygen was monitored the fluorescence of the C4a-hydroxyflavin with excitation wavelength of 380 nm and used optical filter for collecting emission intensity greater than 445 nm. The kinetic race from fluorescence showed formation and decay of the C4a-hydroxyflavin intermediate (red line, Figure 18A). The decay of fluorescence of C4a-hydroxyflavin was the same exponential phase of the flavin oxidation.

The formation of C4a-hydroxyflavin was an exponential phase for hydroxylation of indole to form 3-hydroxyindole whereas the C4a-hydroperoxyflavin was changed to be C4a-hydroxyflavin. An increase in fluorescence was correlated with C4a-formation and decay indicating that the rate hydroxylation was slower than C4a-hydroperoxyflavin but faster than flavin oxidation. The kinetic traces of C4a-hydroxyflavin formation showed dependent on oxygen concentrations (Figure 18B). The results indicated that the rate constant for hydroxylation was partially limited by hydroperoxyflavin formation. Kinetic analysis of C4a-hydroxyflavin for formation at 50% oxygen buffer was 51 ± 0.12 s^{-1}.
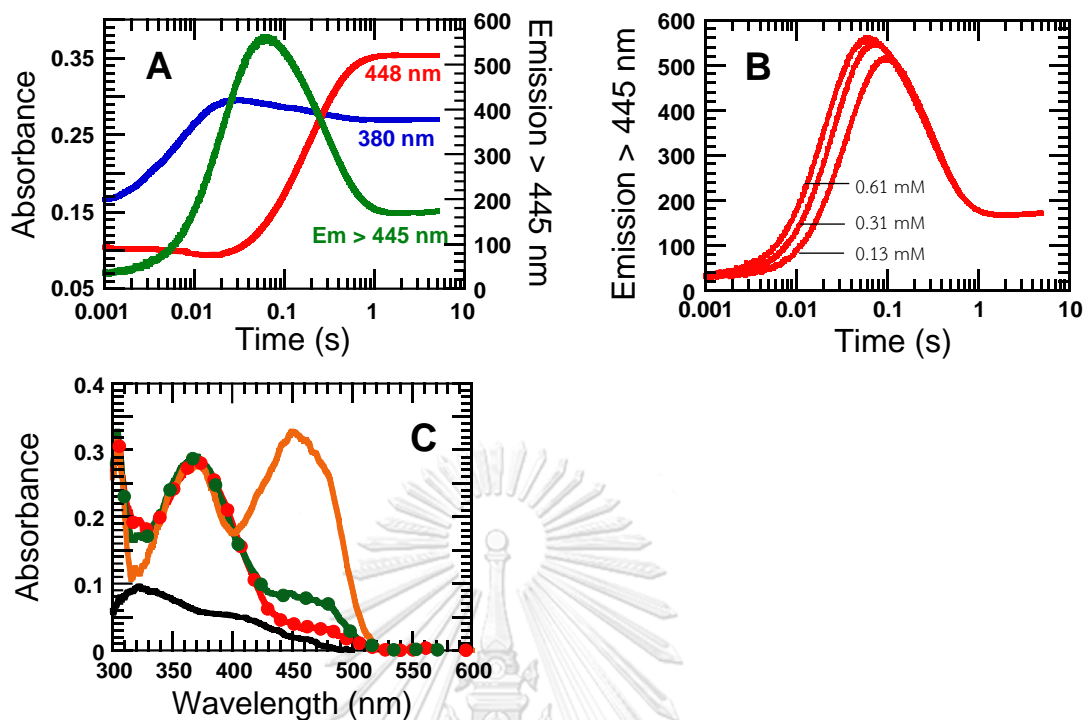
Figure 18. Determination of the hydroxylation rate constant to form 3-hydroxyindole.

A) 30 µM FAD was mixed with IndOx plus 1 mM indole in 0.61 mM oxygen buffer (red line). 30 µM FAD was mixed with IndOx without indole in air-saturation buffer (blue line). The reaction was monitored at 380 nm for C4a-hydroperoxyflavin (blue line) and 448 nm (red line) for flavin oxidation. The fluorescence mode was used to detect emission intensity ≥ 445 nm of C4a-hydroxyflavin with excitation at 380 nm (green line). **B**) The same reaction of A was monitored emission intensity with different oxygen concentrations: 0.13 mM, 0.31 mM, and 0.61 mM (from right to left). **D**) The absorption spectra from 30 µM FADH⁻ was mixed with 150 µM IndOx plus 1 mM indole in 0.62 mM oxygen buffer. The reduced FAD (black line) in presence of IndOx was oxidized to form intermediate (dotted-red line), C4a-hydroxyflavin (dotted-green line) and then decayed to oxidized flavin (blue line).

The CCD detection for spectra change from reduced FAD (black line, Figure 18C). The intermediate C4a-hydroperoxyflavin was presented as dotted-red line. After hydroxylation, the C4a-hydroperoxyflavin was changed to be C4a-hydroxyflavin as dotted-green line (Figure 18C). An increase in absorbance in range of 430 – 500 nm of dotted-green line spectrum was for oxidized flavin around 27%. This showed the percentage of uncoupling path for decay of C4a-hydroxyflavin without hydroxylation to form oxidized flavin and H_2O_2 (orange line, Figure 18C). The reaction mechanism for hydroxylation was represented in Figure 19.
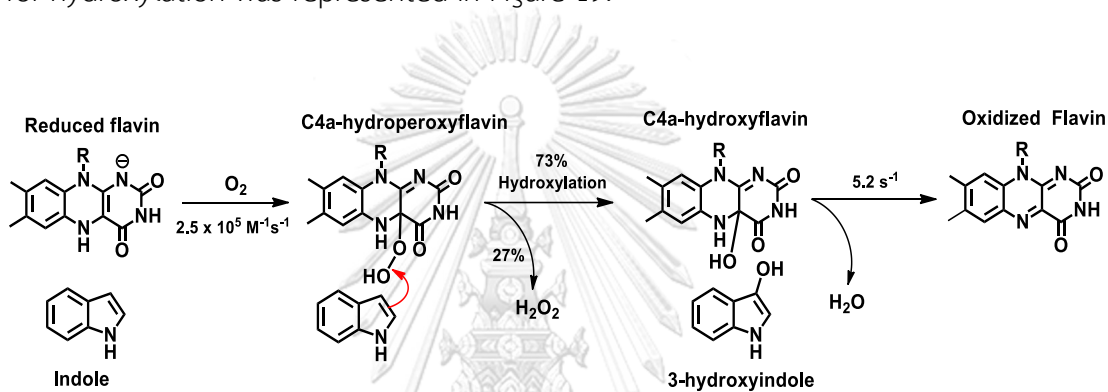

Figure 19. The reaction mechanism of IndOx for hydroxylation of indole.

3.10 The binding of oxidized FAD to IndOx and binding FAD-IndOx complex to indole

The binding of oxidized FAD to IndOx was monitored using an increase in emission intensity of FAD. The fixed concentration of FAD 10 µM was titrated with varied concentrations of IndOx. The dotted-blue line was emission of free FAD. The titration of FAD with IndOx showed an increase in fluorescence as shown in solid line. A plot of FAD-IndOx complex ([ES]) versus IndOx. The binding curve was fit according to Equation 3. to obtain K_d value of 105 ± 2 µM (Figure 20B).

The binding of indole to FAD-IndOx complex was monitored using fluorescence quenching. The dotted-red line was emission spectrum of FAD-IndOx complex. When indole was titrated into the complex, the emission spectra were presented in solid-red lines. A plot of FAD-IndOx-indole complex ([ES]) versus Indole The binding curve was fit according to Equation 3. to obtain K_d value of 0.90 ± 0.02 mM (Figure 20D).
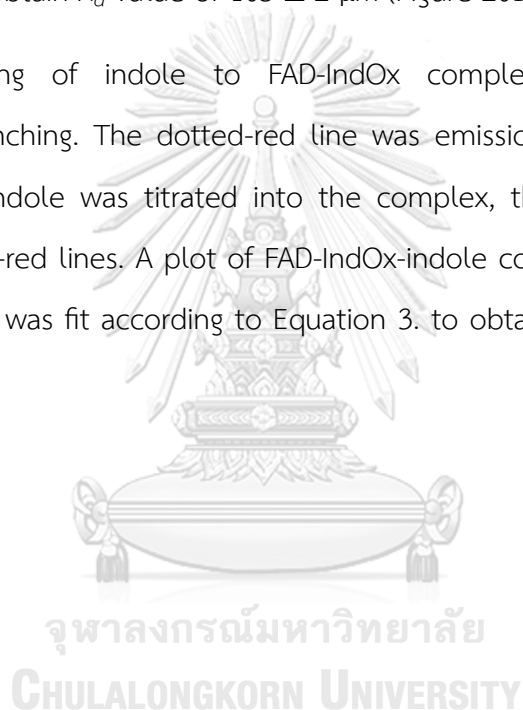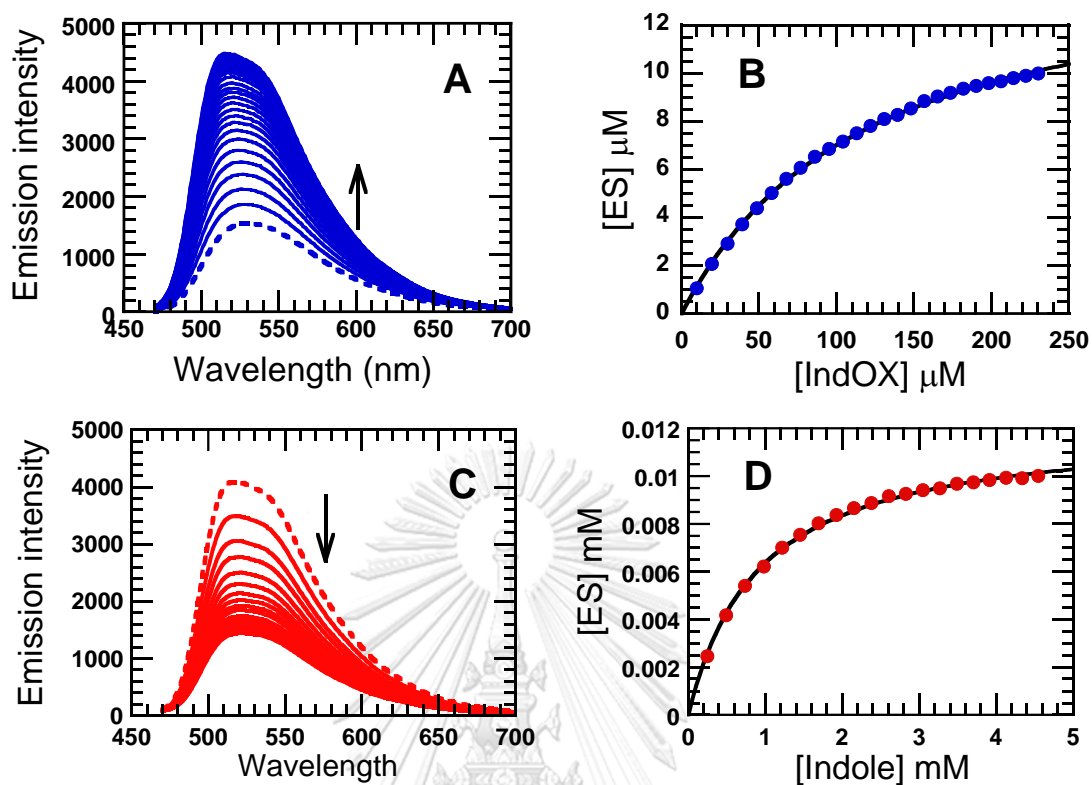
Figure 20. The binding of IndOx to oxidized FAD and the binding of FAD-IndOx complex to indole.

A) 10 μM FAD was titrated with 9 μM – 230 μM of IndOx. The binding of IndOx to FAD resulted in increasing in emission intensity. **B)** A plot of concentrations of FAD-IndOx complex ([ES]) versus IndOx concentrations. **C)** 10 μM FAD in presence of 600 **μ**M was titrated with varied concentrations of indole. The binding of IndOx to FAD resulted in quenching in emission intensity. **D)** A plot of concentrations of ternary complex of FAD-IndOx-indole ([ES]) versus indole concentrations.

3.11 Kinetic reduction of IndR

The kinetic reduction of IndR was investigated by mixing oxidized enzyme in anaerobic close container (tonometer) with varied NADH concentrations. The reduction was monitored with a decrease in absorbance at 456 nm for flavin reduction (blue lines, Figure 21). The results showed a fast decrease in absorbance with the absorbance at 0.002 s around 0.2 indicating that some enzyme population was reduced by NADH before dead time of stopped-flow machine whereas the absorbance of oxidized IndR at 456 nm was around 0.3 (inset Figure 21). The observed rate constants for reduction were not dependent on NADH concentration. These results demonstrated that the K_d between NADH and oxidized IndR for NADH possibly the K_d was very tight.

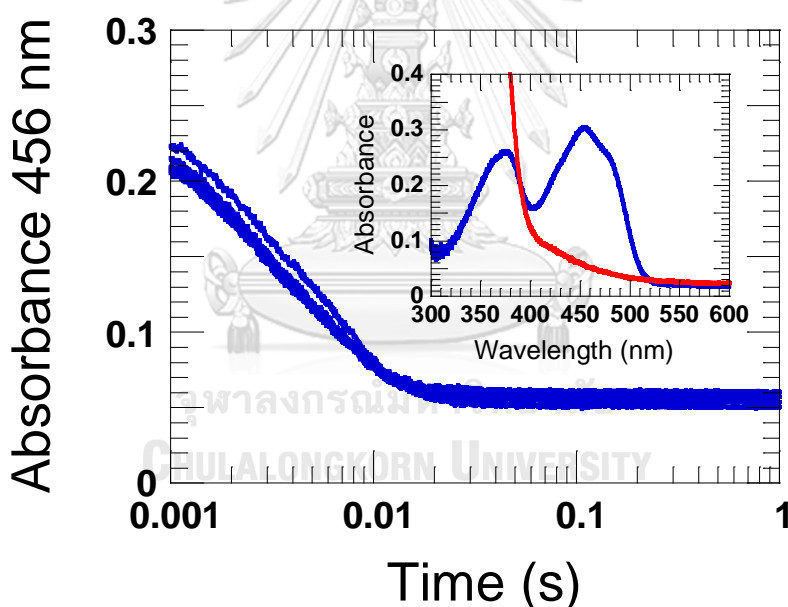**Figure 21. Kinetic reduction of IndR.**

25 μM IndR was mixed with varied NADH concentrations of 0.15,0.3, 0.6, 1.2 and 2.4 mM. The enzyme was reduced with a decrease in absorbance in range of 400 – 500 nm for flavin reduction from blue line to be red line (inset). The reactions were monitored at 456 nm. All kinetic traces were superimposed indicating the reduction was not dependent on NADH concentrations.

3.12 The rate constant of hydroxylation

The rate constant of indole was investigated by mixing oxidized FAD in an anaerobic closed container (glove box) with 25 mM dithionite and quenching it with 0.075 M HCl. After mixing, 25 mM DTT was added to preserve the 3-hydroxyindole for HPLC analysis. The 3-hydroxyindole was monitored at 378 nm. The results showed that the rate of hydroxylation was 47.362 s^{-1} per 0.13 mM oxygen, and the time difference in the concentration of 3-hydroxyindole changed at 0.1 s. (Figure 22.)
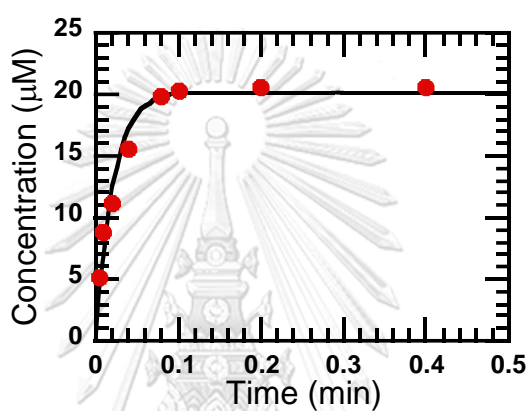
Figure 22. Hydroxylation rate constant of indole

The concentrations of 3-hydroxyindole were changed at 0.1 second. The rate constant was determined from slope of hyperbolic curve.

3.13 The binding of oxygenase component to indole

The isothermal calorimetry titration experiment was performed to investigate the thermodynamic properties of the system. The reaction between 150 µM IndOx and 1 mM indole was studied by monitoring the heat flow during the titration process. The heat flow data obtained during the titration were analyzed to determine the enthalpy change (ΔH) was -4.75 ± 1.19 kcal/mol and the binding constant (K) was 180 ± 83 µM of the interaction between IndOx and indole (Figure 23A). The titration curve exhibited distinct exothermic peaks (Figure 23B), indicating an exothermic binding process.

Figure 23. The isothermal calorimetry titration of the interaction between IndOx and indole

A) Gibbs Free Energy was the thermodynamic quantity of a system was negative (ΔG < 0) for a spontaneous process. **B)** The titration curve exhibited distinct exothermic peaks, indicating an exothermic binding process.
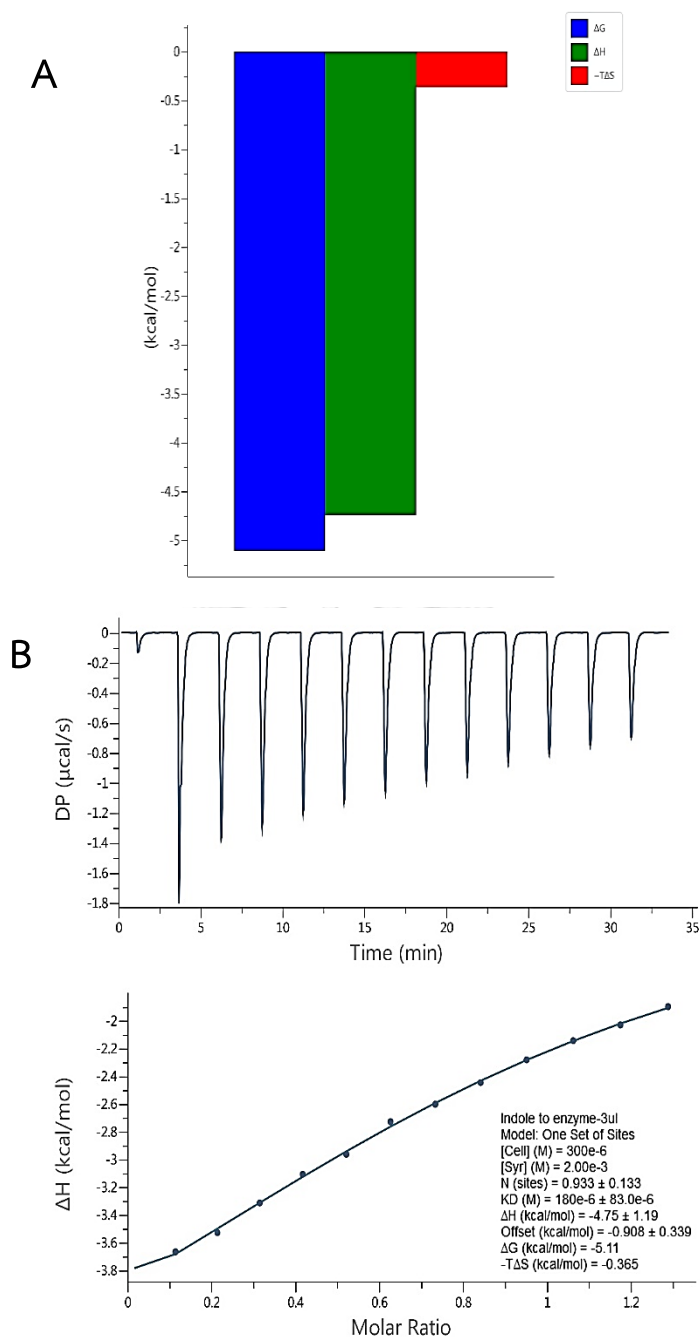
CHAPTER IV

DISCUSSION

Microorganisms expressing monooxygenase activity were selected through recombinant plasmid transformation due to the production of indigo, a dark blue chemical that could be easily observed on agar or in the medium (Arora et al., 2015). Additionally, we found small patches of indigo in our medium. These microorganisms were extensively studied to explore alternative techniques for indigo production (Arora et al., 2015). However, obtaining precise rates of indigo synthesis from the existing literature posed a challenge because the mechanism of indigo production remained uncertain. Therefore, it was necessary for our study to accurately understand the kinetic mechanism of indole monooxygenase in hydroxylation and flavin oxidation. Before investigating or analyzing the mechanism of indigo formation, we wanted to determine the molecular weight and size of IndOx and IndR using the fast protein liquid chromatography. We compared their sizes, with IndOx being 47 kD, it was homodimer like Styrene monooxygenase (StyA1) (Tischler et al., 2010) and IndR being 19 kD, which is similar in size to the oxygenase and reductase derived from *A. baumannii* and *P. putida*. These two enzymes exhibit a two-component enzyme kinetic (Sucharitakul et al., 2007).

Our research focused on investigating the kinetic mechanism of the indole monooxygenase system, which is a two-component flavin-dependent monooxygenase found in *A. baumannii*. We examined both the monooxygenase component (IndOx) and the reductase component (IndR). Through functional studies, we successfully demonstrated the catalytic addition of molecular oxygen to the indole substrate. Furthermore, we developed a method using HPLC for the identification of 3-hydroxyindole. We conducted rapid kinetic analyses using stopped-flow techniques, which revealed the presence of a flavin adduct intermediate involved in the monooxygenation process following substrate cleavage.

To study the rate of the enzymatic reaction of the flavin-dependent monooxygenase group, changes in both absorption and fluorescence of C4a-hydroperoxyflavin were observed. This allowed us to determine the rate constant for the transition from reduced FAD to oxidized FAD by comparing reactions involving both substrate and non-substrate conditions. In the presence of indole, hydroperoxyflavin containing indole FAD underwent conversion to oxidized FAD in approximately 0.03 s. In contrast, the reaction without indole showed the onset of oxidized FAD formation at around 4 s. This difference indicated a 130-fold variation in the reaction compared to C4a-hydroperoxyflavin containing indole-3-pyruvate (IPA), which is a reaction catalyzed by *Arabidopsis* YUCCA flavin-containing monooxygenase. When IPA was present, the conversion to oxidized FAD occurred in approximately 0.56 s, whereas without IPA, the change was observed in only 0.14 s. Consequently, our enzymes exhibited a greater sensitivity to the presence of the reaction substrate, leading to more efficient transformation of FAD compared to *Arabidopsis* enzymes (Cheng et al., 2006).

The results obtained from single-turnover experiments clearly indicated that the oxidation of reduced FAD on IndOx played a crucial role in catalytically cleaving the indole, resulting in the production of 3-hydroxyindole. The use of rapid quenched-flow techniques allowed us to determine that the rate constant observed for the formation of the product, 3-hydroxyindole, was nearly equal to the difference in rate constants between the oxidation of FAD bound to IndOx. However, due to the absence of temperature demonstration in the rapid quenched-flow experiments, further analysis is required to fully understand the temperature dependence of these processes.

It is known that following the redox mechanism of reductase (IndR) and monooxygenase (IndOx), the specific product obtained is 3-hydroxyindole. The dimerization reaction of 3-hydroxyindole was therefore investigated using the multiple turnover technique. It was found that we could produce 13.21 µM/ 5 mL or

692.92 mg/L of indigo, which is a significant increase compared to the 23.60 mg/L obtained by the recombinant strain 4-01 from *Pseudomonas* (Comai & Kosuge, 1982) and the 3.54 mg/L reported in previous studies (Barlier et al., 2000).

The formation of C4a-hydroxyflavin followed an exponential phase during the hydroxylation of indole, resulting in the formation of 3-hydroxyindole. In our study, a similar intermediate to C4a-hydroxy-FAD, which is a product of the epoxidation reaction in styrene monooxygenase, was measured. The observed rate constant for this step was 49.7 ± 0.3 s^{-1}, which was found to be indistinguishable from the rate of the hydride-transfer reduction reaction. This finding is consistent with our kinetic analysis of C4a-hydroxyflavin formation, which yielded a rate constant of 51 ± 0.12 s^{-1}. Therefore, the rates of these reactions were quite similar (Morrison et al., 2013). The binding of IndOx with indole using isothermal calorimeter titration showed exothermic peaks. However, the plot of energy with indole concentrations was not clear for K_d analysis. Therefore, the titration experiment needed to be optimized.

CHAPTER V

CONCLUSION

The recombinant indole monooxygenase component (IndOx) and reductase component (IndR) enzymes, both tagged with C-terminal histidine, were successfully expressed in *E. coli* and obtained as soluble proteins. After purification, the yields of pure proteins were approximately 0.31 g/L and 0.11 g/L of cell culture for IndOx and IndR, respectively. Size-exclusion chromatography on an FPLC system was utilized to determine the native molecular weights of both IndOx and IndR. The results indicated that IndOx exists as a dimer, while IndR forms a monomer. During the cofactor analysis of IndR, it was discovered that FAD constituted 99.09%. This indicates that FAD is the primary cofactor utilized by IndR. In the kinetic assay, FAD was predominantly employed as the cofactor. A rapid kinetic study confirmed the stabilization of the C4a-hydroperoxyflavin spectrum during the oxidation kinetics of IndOx. Product analysis using HPLC revealed specific hydroxylation of the indole substrate at C3 by the enzyme. Moreover, the presence of indigo product resulting from the atmospheric oxygenation of 3-hydroxyindole was also detected in the HPLC analysis. These findings highlight the enzyme's significant potential for biotechnological applications, particularly in the production of indigo dye.

REFERENCES

Abdurachim, K., & Ellis, H. R. (2006). Detection of protein-protein interactions in the alkanesulfonate monooxygenase system from *Escherichia coli*. *Journal of Bacteriology*, **188**, 8153-8159.

Antunes, L. C., Imperi, F., Carattoli, A., & Visca, P. (2011). Deciphering the multifactorial nature of *Acinetobacter baumannii* pathogenicity. *Plos One*, **6**, e22674.

Arora, P. K., Sharma, A., & Bae, H. (2015). Microbial degradation of indole and Its derivatives. *Journal of Chemistry*, **2015**, 129159.

Barlier, I., Kowalczyk, M., Marchant, A., Ljung, K., Bhalerao, R., Bennett, M., Sandberg, G., & Bellini, C. (2000). The SUR2 gene of *Arabidopsis* thaliana encodes the cytochrome P450 CYP83B1, a modulator of auxin homeostasis. *Proceedings of the National Academy of Sciences*, **97**, 14819-14824.

Céspedes, C. L., Alarcon, J., Valdez-Morales, M., & Paredes-López, O. (2009). Antioxidant activity of an unusual 3-hydroxyindole derivative isolated from fruits of Aristotelia chilensis (Molina) Stuntz. *Zeitschrift für Naturforschung C*, **64**, 759-762.

Cheng, Y., Dai, X., & Zhao, Y. (2006). Auxin biosynthesis by the YUCCA flavin monooxygenases controls the formation of floral organs and vascular tissues in *Arabidopsis*. *Genes & Development*, **20**, 1790-1799.

Chenprakhon, P., Wongnate, T., & Chaiyen, P. (2019). Monooxygenation of aromatic compounds by flavin-dependent monooxygenases. *Protein Science*, **28**, 8-29.

Comai, L., & Kosuge, T. (1982). Cloning characterization of iaaM, a virulence determinant of *Pseudomonas savastanoi*. *Journal of Bacteriology*, **149**, 40-46.

Dai, C., Ma, Q., Li, Y., Zhou, D., Yang, B., & Qu, Y. (2019). Application of an efficient indole oxygenase system from *Cupriavidus* sp. SHE for indigo production. *Bioprocess and Biosystems Engineering*, **42**, 1963-1971.

De Boer, L. (2014). Biotechnological production of colorants. *Advances in Biochemical Engineering/Biotechnology*, **143**, 51-89.

Fabara, A. N., & Fraaije, M. W. (2020). An overview of microbial indigo-forming enzymes. *Applied Microbiology and Biotechnology*, **104**, 925-933.

Fetzner, S. (1998). Bacterial degradation of pyridine, indole, quinoline, and their derivatives under different redox conditions. *Applied Microbiology and Biotechnology, 49*, 237-250.

Gillam, E. M., Notley, L. M., Cai, H., De Voss, J. J., & Guengerich, F. P. (2000). Oxidation of indole by cytochrome P450 enzymes. *Biochemistry, 39*, 13817-13824.

Grabski, A., Mehler, M., & Drott, D. (2005). The overnight express autoinduction system: high-density cell growth and protein expression while you sleep. In: *Nature Publishing Group*.

Groeneveld, M., Van Beek, H., Duetz, W., & Fraaije, M. (2016). Identification of a novel oxygenase capable of regiospecific hydroxylation of D-limonene into (+)-trans-carveol. *Tetrahedron, 72*, 7263-7267.

Gu, J.-D., & Berry, D. F. (1992). Metabolism of 3-methylindole by a methanogenic consortium. *Applied and Environmental Microbiology, 58*, 2667-2669.

Han, G. H., Gim, G. H., Kim, W., Seo, S. I., & Kim, S. W. (2012). Enhanced indirubin production in recombinant *Escherichia coli* harboring a flavin-containing monooxygenase gene by cysteine supplementation. *Journal of Biotechnology, 164*, 179-187.

Hsu, T. M., Welner, D. H., Russ, Z. N., Cervantes, B., Prathuri, R. L., Adams, P. D., & Dueber, J. E. (2018). Employing a biochemical protecting group for a sustainable indigo dyeing strategy. *Nature Chemical Biology, 14*, 256-261.

Iwahana, S., Iida, H., Yashima, E., Pescitelli, G., Di Bari, L., Petrovic, A. G., & Berova, N. (2014). Absolute stereochemistry of a 4 a-hydroxyriboflavin analogue of the key intermediate of the FAD-monooxygenase cycle. *Chemistry, 20,* 4386-4395.

Johnson, C. M. (2021). Isothermal titration calorimetry. *Methods in Molecular Biology, 2263*, 135-159.

Lai, C.-C., & Chang, C.-E. (2021). A study on sustainable design for indigo dyeing color in the visual aspect of clothing. *Sustainability, 13*, 3686.

Lee, J.-H., & Lee, J. (2010). Indole as an intercellular signal in microbial communities. *FEMS Microbiology Reviews, 34*, 426-444.

Lin, G. H., Chen, H. P., & Shu, H. Y. (2015). Detoxification of indole by an indole-induced

flavoprotein oxygenase from *Acinetobacter baumannii*. *Plos One*, **10**, e0138798.

Madadlou, A., O'Sullivan, S., & Sheehan, D. (2011). Fast protein liquid chromatography. *Methods in Molecular Biology*, **681**, 439-447.

Mascotti, M. L., Ayub, M. J., Furnham, N., Thornton, J. M., & Laskowski, R. A. (2016). Chopping and changing: the evolution of the flavin-dependent monooxygenases. *Journal of Molecular Biology*, **428**, 3131-3146.

Meyer, A., Wu, M., Schmid, A., Kohler, H.-P. E., & Witholt, B. (2002). Hydroxylation of indole by laboratory-evolved 2-hydroxybiphenyl 3-monooxygenase. *Journal of Biological Chemistry*, **277**, 34161-34167.

Mohammed, N., Onodera, R., & Or-Rashid, M. (2003). Degradation of tryptophan and related indolic compounds by ruminal bacteria, protozoa and their mixture in vitro. *Amino Acids*, **24**, 73-80.

Morrison, E., Kantz, A., Gassner, G. T., & Sazinsky, M. H. (2013). Structure and mechanism of styrene monooxygenase reductase: new insight into the FAD-transfer reaction. *Biochemistry*, *52*, 6063-6075.

O'Connor, K. E., Dobson, A., & Hartmans, S. (1997). Indigo formation by microorganisms expressing styrene monooxygenase activity. *Applied and Environmental Microbiology*, *63*, 4287-4291.

Panke, S., Witholt, B., Schmid, A., & Wubbolts, M. G. (1998). Towards a biocatalyst for (S)-styrene oxide production: characterization of the styrene degradation pathway of *Pseudomonas* sp. strain VLB120. *Applied and Environmental Microbiology*, *64*, 2032-2043.

Parales, R. E., Ontl, T. A., & Gibson, D. T. (1997). Cloning and sequence analysis of a catechol 2,3-dioxygenase gene from the nitrobenzene-degrading strain *Comamonas* sp JS765. *Journal of Industrial Microbiology and Biotechnology*, *19*, 385-391.

Paul, C. E., Eggerichs, D., Westphal, A. H., Tischler, D., & van Berkel, W. J. H. (2021). Flavoprotein monooxygenases: versatile biocatalysts. *Biotechnology Advances*, *51*, 107712.

Pimviriyakul, P., Surawatanawong, P., & Chaiyen, P. (2018). Oxidative dehalogenation and denitration by a flavin-dependent monooxygenase is controlled by substrate

deprotonation. *Chemical Science*, *9*, 7468-7482.

Qin, Z., Wang, X., Gao, S., Li, D., & Zhou, J. (2023). Production of natural pigments using microorganisms. *Journal of Agricultural and Food Chemistry*, *71*, 9243-9254.

Sheng, D., Ballou, D. P., & Massey, V. (2001). Mechanistic studies of cyclohexanone monooxygenase: chemical properties of intermediates involved in catalysis. *Biochemistry*, *40*, 11156-11167.

Sucharitakul, J., Buckel, W., & Chaiyen, P. (2021). Rapid kinetics reveal surprising flavin chemistry in bifurcating electron transfer flavoprotein from *Acidaminococcus fermentans*. *Journal of Biological Chemistry*, *296*, 100124.

Sucharitakul, J., Phongsak, T., Entsch, B., Svasti, J., Chaiyen, P., & Ballou, D. P. (2007). Kinetics of a two-component *p*-hydroxyphenylacetate hydroxylase explain how reduced flavin is transferred from the reductase to the oxygenase. *Biochemistry*, *46*, 8611-8623.

Sucharitakul, J., Prongjit, M., Haltrich, D., & Chaiyen, P. (2008). Detection of a C4a-hydroperoxyflavin intermediate in the reaction of a flavoprotein oxidase. *Biochemistry*, *47*, 8485-8490.

Sumpter W. C., M. F. M. (1954). *Heterocyclic compounds with indole and carbazole systems*. Wiley-Interscience.

Tischler, D., Kermer, R., Gröning, J. A., Kaschabek, S. R., van Berkel, W. J., & Schlömann, M. (2010). StyA1 and StyA2B from *Rhodococcus opacus* 1CP: a multifunctional styrene monooxygenase system. *Journal of Bacteriology*, *192*, 5220-5227.

Van Berkel, W., Kamerbeek, N., & Fraaije, M. (2006). Flavoprotein monooxygenases, a diverse class of oxidative biocatalysts. *Journal of Biotechnology*, *124*, 670-689.

van Hellemond, E. W., Janssen, D. B., & Fraaije, M. W. (2007). Discovery of a novel styrene monooxygenase originating from the metagenome. *Applied and Environmental Microbiology*, *73*, 5832-5839.

Yokoyama, M., & Carlson, J. (1974). Dissimilation of tryptophan and related indolic compounds by ruminal microorganisms in vitro. *Applied Microbiology*, *27*, 540-548.

Yuan, L.-J., Liu, J.-B., & Xiao, X.-G. (2011). Biooxidation of indole and characteristics of

the responsible enzymes. *African Journal of Biotechnology, **10**,* 19855-19863.

VITA

NAME	Kanyarat Suksomjaisaman
DATE OF BIRTH	6 March 1997
PLACE OF BIRTH	Thailand
INSTITUTIONS ATTENDED	B.Sc. Kasetsart University
HOME ADDRESS	16/5 Moo.11 Bangnumphueng Phrapraaeng Samutprakan 10130
PUBLICATION	Kanyarat Suksomjaisaman, Supaart Sirikantaramas, and Jeerus Sucharitakul. (2022). Heterologous production of two-component flavin-dependent indole monooxygenase from Acinetobacter baumannii. In the 17th International Symposium Of The Protein Society of Thailand

จุฬาลงกรณ์มหาวิทยาลัย
CHULALONGKORN UNIVERSITY